REVERSE KINEMATIC ANALYSIS AND UNCERTAINTY ANALYSIS OF THE SPACE SHUTTLE AFT PROPULSION SYSTEM (APS) POD LIFTING FIXTURE

By

JEFFREY S. BRINK

A THESIS PRESENTED TO THE GRADUATE SCHOOL
OF THE UNIVERSITY OF FLORIDA IN PARTIAL FULFILLMENT
OF THE REQUIREMENTS FOR THE DEGREE OF
MASTER OF ENGINEERING

UNIVERSITY OF FLORIDA

2004

This thesis is dedicated to the Kennedy Space Center workers that have done their best to help this effort succeed in hopes of making operations better and safer.

ACKNOWLEDGMENTS

The author would like to thank NASA Orbiter Handling Rob Summers and USA Orbiter Handling Glenn Roberts for their invaluable help. As the experts on this hardware and installation process, they responded promptly and patiently to my constant barrage of questions. Their willingness to do anything they can to make operations safer is commendable. They shoot a pretty good game of pool, too.

Boeing Orbiter Handling Will Judd was also very helpful. He answered several technical questions and verified the accuracy of some information I had found on my own.

NASA Payload Mechanical Engineering Doug Lenhardt and NASA Mechanical Design Engineer Paul Schwindt were instrumental in the Pro/E portion of this study. Doug and Paul answered questions that helped my knowledge of Pro/E grow from beginner level to intermediate.

After experiencing quite a bit of difficulty getting the integrated C program to run, NASA Senior Software Engineer Dan Nieten was kind enough to teach the author several very helpful debugging techniques. These techniques enabled the author to figure out what was wrong and how to make it work.

NASA Thermal Protection Systems Lisa Huddleston provided guidance on performing my literature review and gave tips on how to use numerical methods to reduce error in the integrated program. I also frequently consulted Lisa about details of

this study and – even though robotics is not her field of expertise - she never seemed to run out of good questions.

The author would also like to thank his thesis committee for their contribution. Dr. Carl Crane III, thesis advisor, was particularly helpful and the concepts taught in his textbook formed the backbone to this solution method. Dr. John Scheuller and Dr. Ashok Kumar provided good insight as this thesis reached its conclusion.

NASA Launch Accessories Kristina Morace and NASA Orbiter Handling Ryan Holmes checked the technical content of this thesis and helped make it more clear and understandable.

TABLE OF CONTENTS

LIST OF TABLES

Table page

LIST OF FIGURES

Figure page

Abstract of Dissertation Presented to the Graduate School
of the University of Florida in Partial Fulfillment of the
Requirements for the Degree of Master of Engineering

REVERSE KINEMATIC ANALYSIS AND UNCERTAINTY ANALYSIS
OF THE SPACE SHUTTLE AFT PROPULSION SYSTEM (APS) POD LIFTING
FIXTURE

By

JEFFREY S. BRINK

APRIL 2005

Chair: Dr. Carl D. Crane III
Major Department: Mechanical and Aerospace Engineering

The space shuttle Aft Propulsion System (APS) pod requires precision alignment to be installed onto the orbiter deck. The ground support equipment used to perform this task can't be manipulated along a single Cartesian axis without causing motion along the other Cartesian axes. As a result, manipulations required to achieve a desired motion are not intuitive. This thesis calculates the joint angles required to align the APS pod using reverse kinematic analysis techniques. Knowledge of these joint angles will allow the shuttle team to align the APS pod more safely and efficiently. An uncertainty analysis has also been performed to estimate the accuracy associated with this approach and to determine whether any inexpensive modifications can be made to further improve accuracy.

CHAPTER 1
BACKGROUND

Introduction

The Kennedy Space Center (KSC) is NASA's "operations center" for the space shuttle. This role includes mission configuration and deconfiguration, vehicle modifications, repair, and routine maintenance – essentially everything that happens to a space shuttle orbiter from landing through launch. The installation of an Aft Propulsion System (APS) pod onto an orbiter is one example of a KSC operation.

This thesis seeks to improve the APS pod installation operation by calculating the joint offsets required to align the APS pod with the orbiter deck. These calculations can be performed before the operation begins, which will reduce the operational time spent performing the alignment. The APS pod installation is classified as a hazardous operation, which makes an operational time reduction particularly desirable. Throughout the operation, the potential exists to develop a hypergol leak that could be lethal to nearby personnel.

The Ground Support Equipment (GSE) used to perform an APS pod installation consists of a lifting fixture, two adjustment mechanisms and rotator bar. There are a total of 13 joints that change position during the operation. This analysis will show that they can be considered as three separate manipulators connected by a large structure. After the desired position of the large structure has been ascertained, the end effector position and orientation of each manipulator is found. A reverse kinematic analysis is then performed for each manipulator to determine joint angles.

An uncertainty analysis was then conducted. Both 100% covariance and Root Sum Squared methods were used to quantify alignment accuracy. This analysis was used to determine whether the solution method described above is accurate enough to aid APS pod installation operations and which error sources can be eliminated for significant improvements in accuracy.

Definitions for acronyms and shuttle-related terms can be found in Appendix A.

Hardware Familiarization

Each space shuttle orbiter has two APS pods, one on each side of the vertical tail. Each APS pod houses the Orbital Maneuvering System (OMS) and the aft Reaction Control System (RCS). OMS is the propulsion system that provides thrust for orbital insertion, orbit circularization, orbit transfer, rendezvous, and deorbit.[12]. RCS is the propulsion system used as the primary flight control at altitudes greater than 70,000 feet.[12] An APS pod can be seen in Figure 1-1.

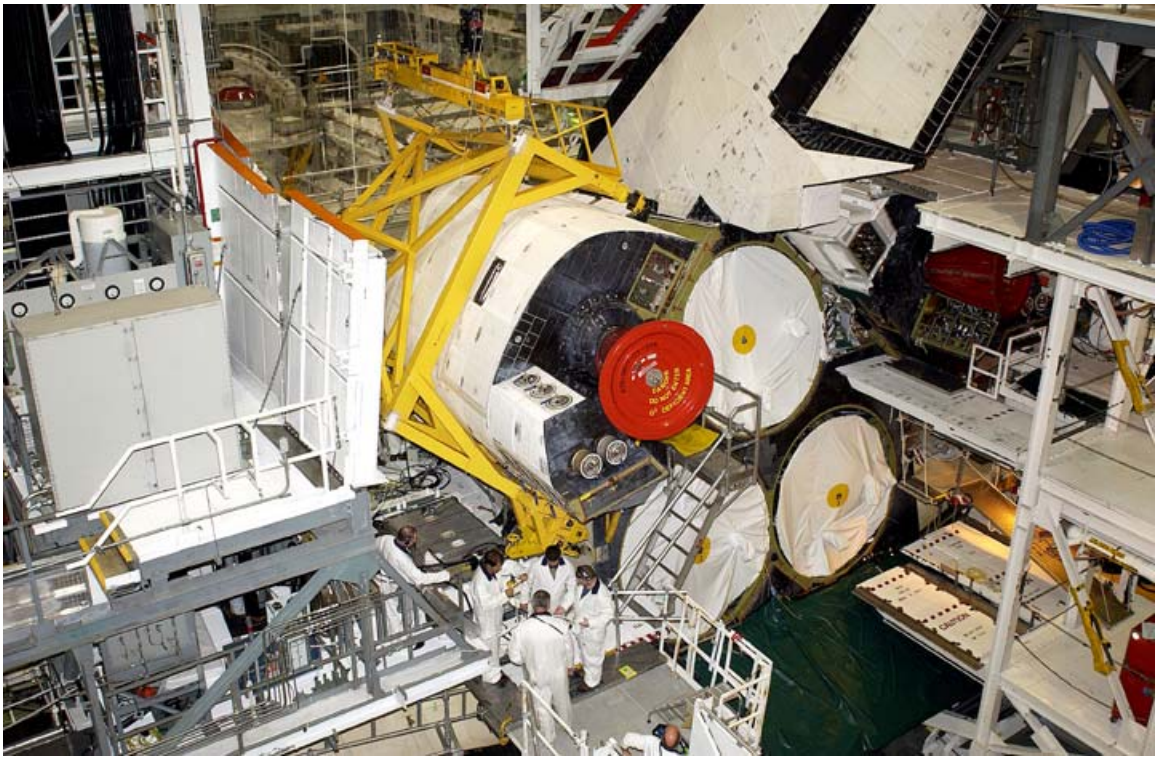

Figure 1-1 - A left APS pod is being removed from the space shuttle orbiter Atlantis.

APS pods were not designed to be maintenanced while installed on an orbiter. As a result, APS pods must be removed for inspections and repairs, generally after every three or four flights. Upon completion of these tasks, the APS pod is installed onto the orbiter.

The APS pod is attached to the orbiter deck at 12 locations called attach points. During the installation operation, all efforts are focused on aligning attach points 1, 2, and 3. If those three attach points are aligned then attach bolts can be installed at all twelve attach point locations. Attach point 1 is the forward inboard attach point, attach point 2 is the forward outboard attach point, and attach point 3 is the aft outboard attach point. Attach point locations are shown in Figure 1-2.

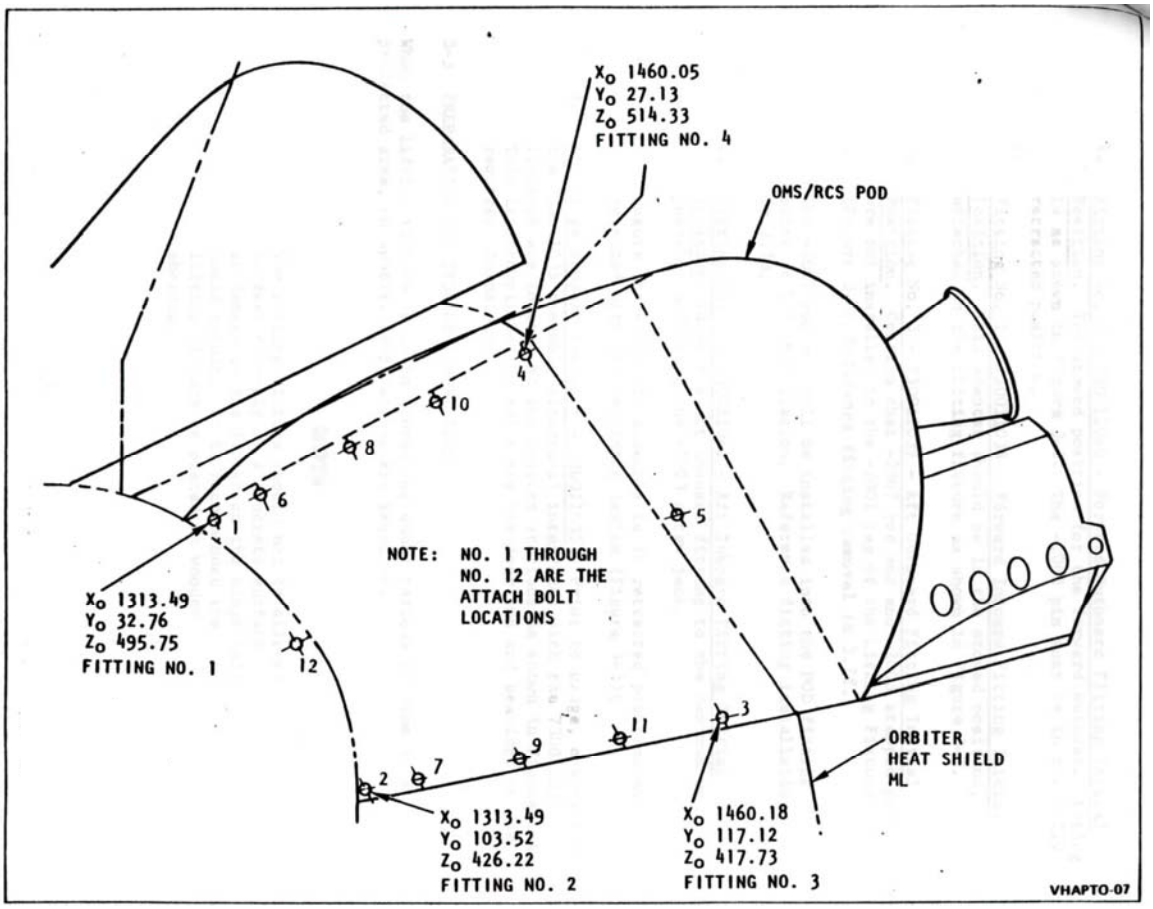

Figure 1-2 - The twelve APS pod attach point locations, left pod shown (right pod mirror).

The APS pod attach point 3 fitting must be aligned within 0.0033" (+/- 0.0018" depending on tolerances) of the orbiter bushing or else the attach bolt can't be installed. The APS pod attach point 2 bushing resides in a slotted hole, which prevents pod-to-pod variation and other factors from making an APS pod "not fit" onto an orbiter. The APS pod attach point 2 fitting must be aligned within 0.0093" +/- 0.0048" in the non-slotted direction. Since attach points 2 and 3 are 12' 3.3" apart, this accuracy requirement is equivalent to positioning attach point 3 within 0.0033" on the orbiter deck and then orienting the APS pod to within 0.0036° of the desired position. The orbiter attach point 1 bushing can accommodate misalignments of up to 0.2190" along the orbiter deck plane.

The alignment process is made significantly more challenging by the presence of a bulb seal on the bottom surface of the APS pod. The bulb seal is basically a hollow flexible tube that forms an environmental seal when compressed against the orbiter deck. When the bulb seal is compressed, the APS pod can't be moved along the orbiter deck plane without risking damage to the bulb seal (the bulb seal is more likely to tear than slide along the deck). As a result, if the APS pod is lowered onto the orbiter deck and discovered to be misaligned then it can't simply be adjusted until it is aligned. Instead, it must be raised off the deck (until the bulb seal is no longer compressed) before it can be adjusted and then lowered onto the orbiter deck.

The ground support equipment used to install APS pods is a lifting fixture, forward adjustment mechanism, aft adjustment mechanism, and rotator bar. These components are labeled in Figure 1-3.

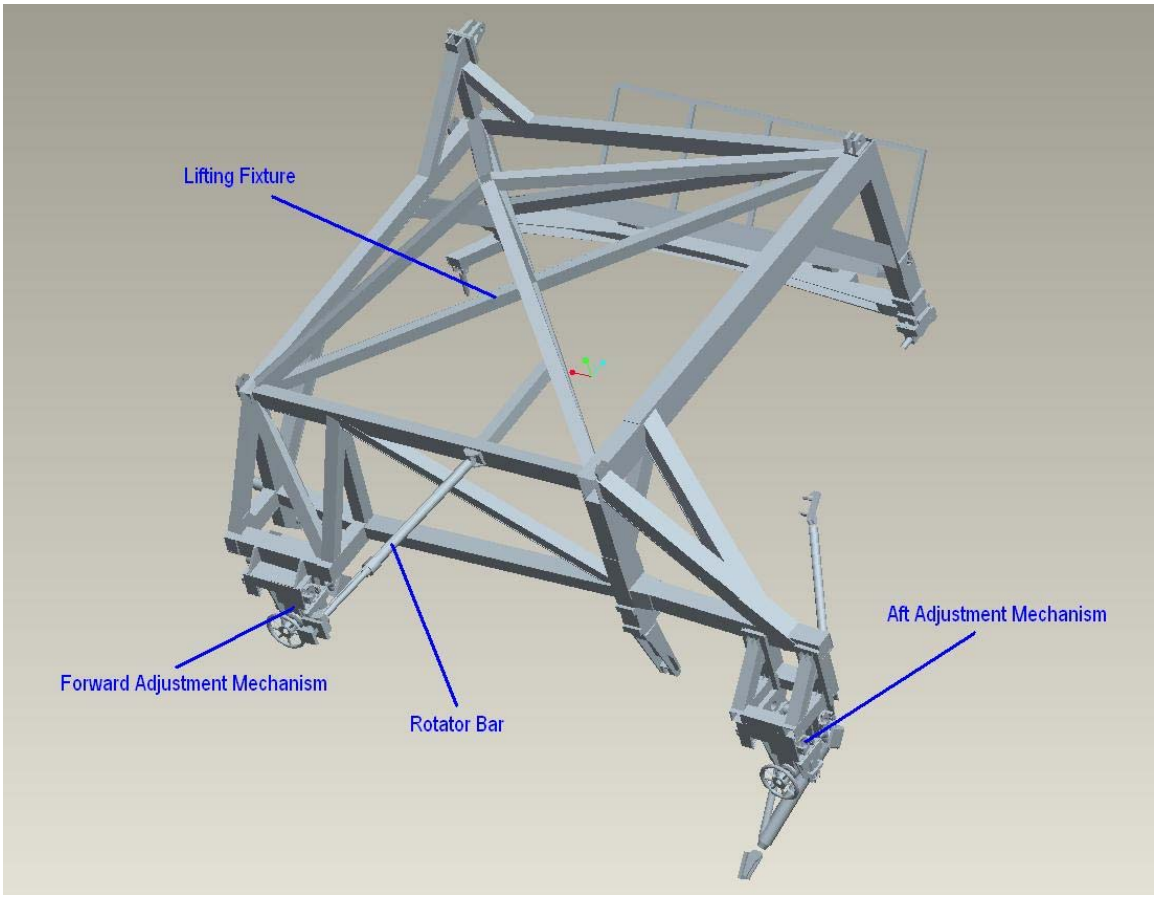

Figure 1-3 - GSE used to install an APS pod.

The lifting fixture is a large structure that connects to the APS pod at APS pod attach point 1, 2, 3, and 4 fittings. The lifting fixture can be adjusted at attach points 1, 2, 3 and 4 to accommodate pod-to-pod dimensional variation. As a result of this adjustment capability, not every APS pod will have the exact same position and orientation relative to the lifting fixture.

The forward and aft adjustment mechanisms structurally support the lifting fixture and allow its position to be adjusted. Forward and aft adjustment mechanisms are nearly identical. Temporary supports are mounted to the orbiter and the adjustment mechanisms each form a spherical joint with a support. Adjustment mechanisms have three

orthogonal prismatic joints that allow motion in the forward/aft, uphill/downhill, and off-the-deck/on-the-deck directions. The lifting fixture is connected to the adjustment mechanisms by the forward/aft prismatic joint. See Figure 1-4 for adjustment mechanism prismatic joint axis directions.

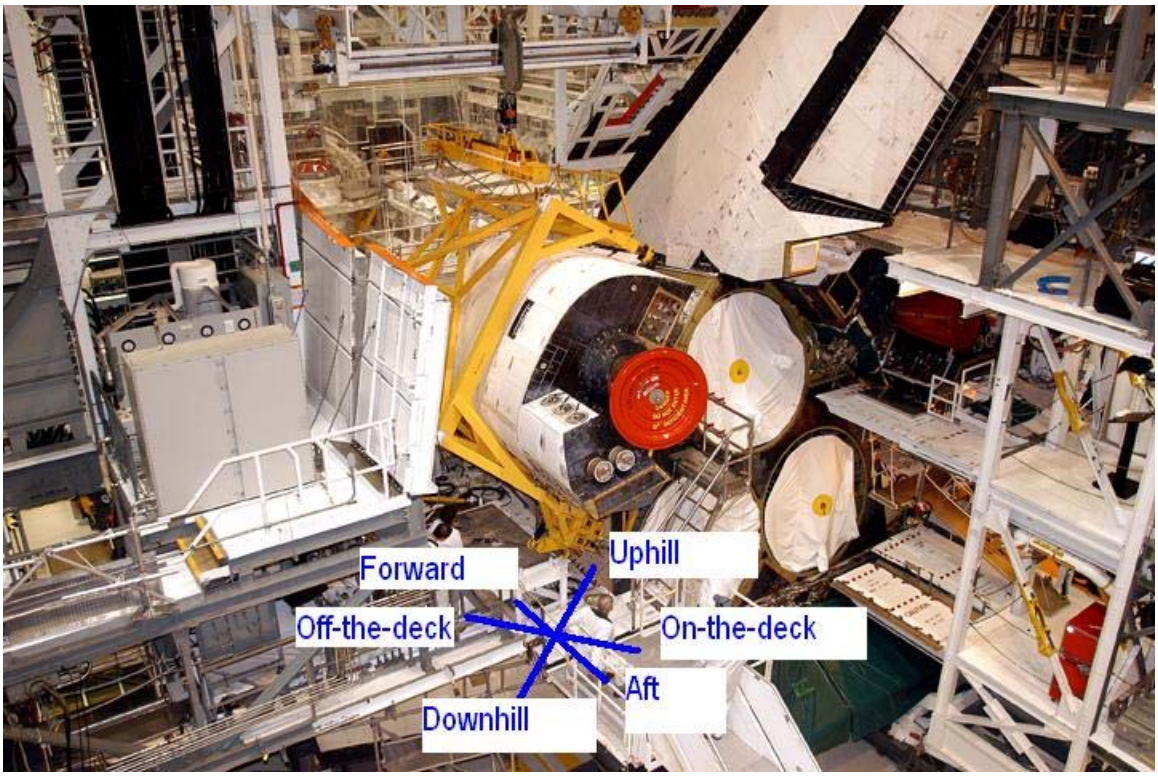

Figure 1-4 - Forward and aft adjustment mechanisms allow motion in forward/aft, uphill/downhill, and off-the-deck/on-the-deck directions.

The center of gravity of the lifting fixture and APS pod is not directly above the spherical joints for the duration of the APS pod installation. As a result, the rotator bar is used to control the rotation of the lifting fixture about the two adjustment mechanism spherical joints (the two spherical joints essentially form a hinge). One end of the rotator bar is rigidly attached to the lifting fixture and the other end is mounted to a large stationary beam. Revolute joints are employed to ensure the rotator bar doesn't restrict the lifting fixture motion. Figure 1-5 shows the rotator bar's revolute joint axes.

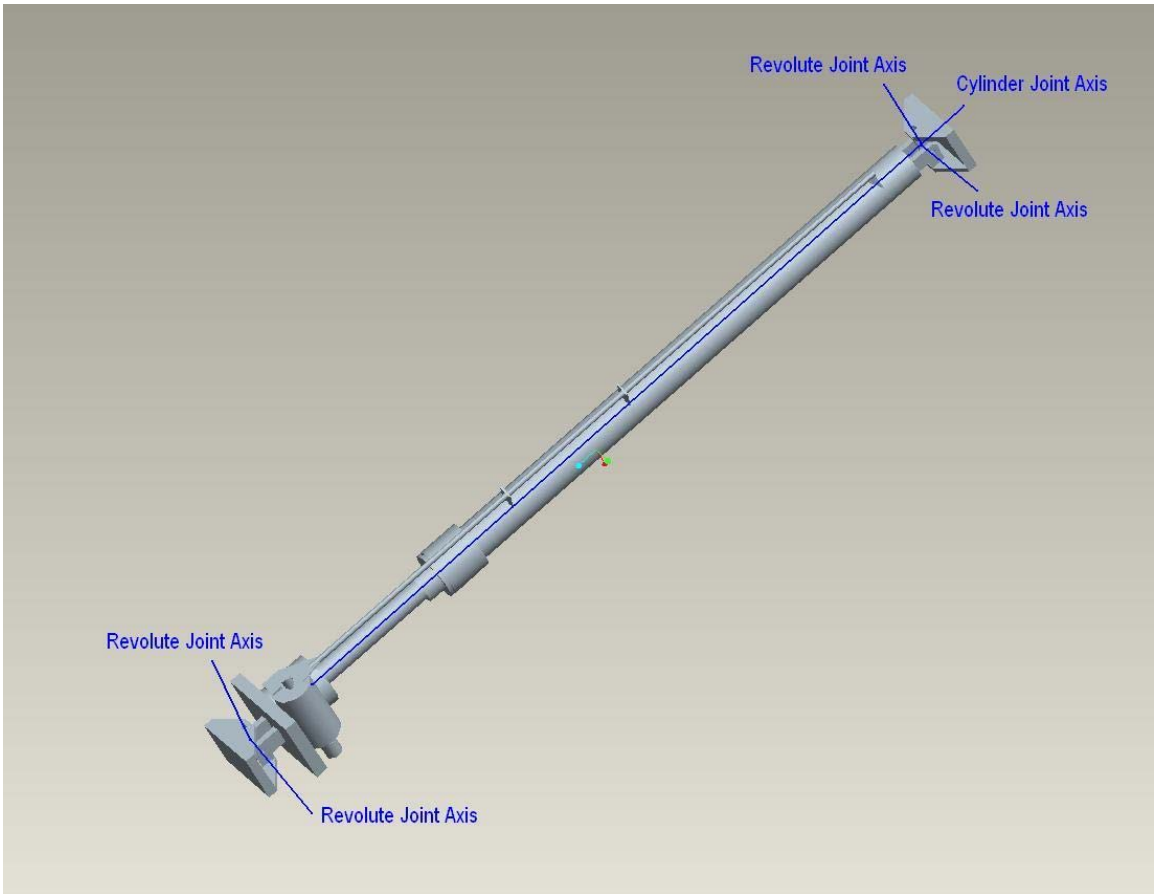

Figure 1-5 - Rotator bar joint axes.

It should be noted that none of the revolute and spherical joints can be actuated. Their role in the alignment process is purely passive.

Installation Procedure and Methodology

The APS pod installation operation begins with the APS pod in the OPF transfer aisle. The lifting fixture, forward adjustment mechanism, and aft adjustment mechanism assembly has already been attached to the APS pod. A bridge crane lifts the APS pod and GSE to a location near the orbiter as shown in Figure 1-6. Adjustment mechanism prismatic joints have been adjusted to provide maximum clearance to the orbiter as the spherical joints are connected. The crane transfers the weight of the APS pod, lifting fixture, and adjustment mechanisms to the spherical joints. The rotator bar is then

extended until it can be connected to the lifting fixture and the alignment portion of this operation begins.

Figure 1-6 - A left APS pod is transported by crane to Atlantis for installation.

According to the APS pod operations and maintenance manual, the rotator bar is extended until the APS pod mating surface is approximately 2.5” above the orbiter deck and the surfaces are parallel. The lifting fixture is moved forward or aft to the “install position” (a marking on the lifting fixture structure). Additional adjustments are made to align attach points 2 and 3. The APS pod is then lowered to 1/8” above the orbiter deck with mating surfaces parallel. The bulb seal is now contacting the orbiter deck but it is not compressed. Adjustments are made again to align attach points 2 and 3. Once aligned, the APS pod is lowered onto the orbiter deck and observers check to make sure the inboard side of the APS pod is also seated. If the APS pod is misaligned, it must be raised off the deck 1/8” or more, adjusted as required, and lowered back onto the deck.

Attach point bolts are installed upon successful completion of the APS pod alignment procedure [14].

APS pod alignment is not accomplished as easily as the operations and maintenance manual describes. It is not possible to adjust the position of one attach point without affecting the position of the other attach points. This is particularly evident when either attach point 2 or 3 has been aligned - adjustments intended to align one attach point usually misalign the other. The person who determines the next manipulation and commands that it be executed is known as the move director. Different move directors have differing philosophies about whether attach point 2 or attach point 3 should be aligned first.

Move directors also use different techniques to align an APS pod. One technique is to align the APS pod 1/8" above the orbiter deck, then simultaneously retract the rotator bar and actuate both adjustment mechanisms in the on-the-deck direction. Another technique is to slightly misalign the APS pod, then allow the rotator bar to correct the misalignment as both adjustment mechanisms are simultaneously adjusted in on-the-deck direction. It should be noted that simultaneous motion is accomplished by manual start/stop and velocity control.

Additionally, not all equipment operates as designed. Field experience has shown that the forward/aft install position does not necessarily align the APS pod. The aft adjustment mechanism's forward/aft prismatic joint wasn't designed with an actuator – it was designed to "follow" the motion of the forward adjustment mechanism. However, it binds rather than follows so a hydraulic jack is used to force it to follow.

The next chapter will present an analytical method used to determine the adjustment mechanism positions and rotator bar position needed to align the APS pod.

CHAPTER 2
PROPOSED ALIGNMENT METHOD

Overview

The geometry of all relevant hardware and the desired position and orientation of the APS pod is known. As a result, a reverse kinematic analysis was conducted to determine sets of joint angles that would align the APS pod with the orbiter.

Due to the large number of joints associated with this hardware, the rotator bar and adjustment mechanisms were treated as three independent robots connected by a large rigid structure. Since the large structure (lifting fixture) has adjustment capability to attach to the APS pod, it is assumed that these adjustments will be measured before the operation begins and is incorporated into the analysis.

The lifting fixture CAD model (see Figure 1-3) shows it in the position required to align the APS pod. As discussed previously, the displayed alignment position doesn't necessarily align the APS pod with the orbiter. The coordinates given in the CAD model were used as a starting point in this analysis. They were used to determine the position and orientation of the three robot end effectors. End effector position and orientation, partnered with known geometry, was used to perform reverse kinematic analyses. The

output of these analyses was the joint angles required to align the APS pod. Figure 2-1 shows the process used to determine the manipulator joint offsets.

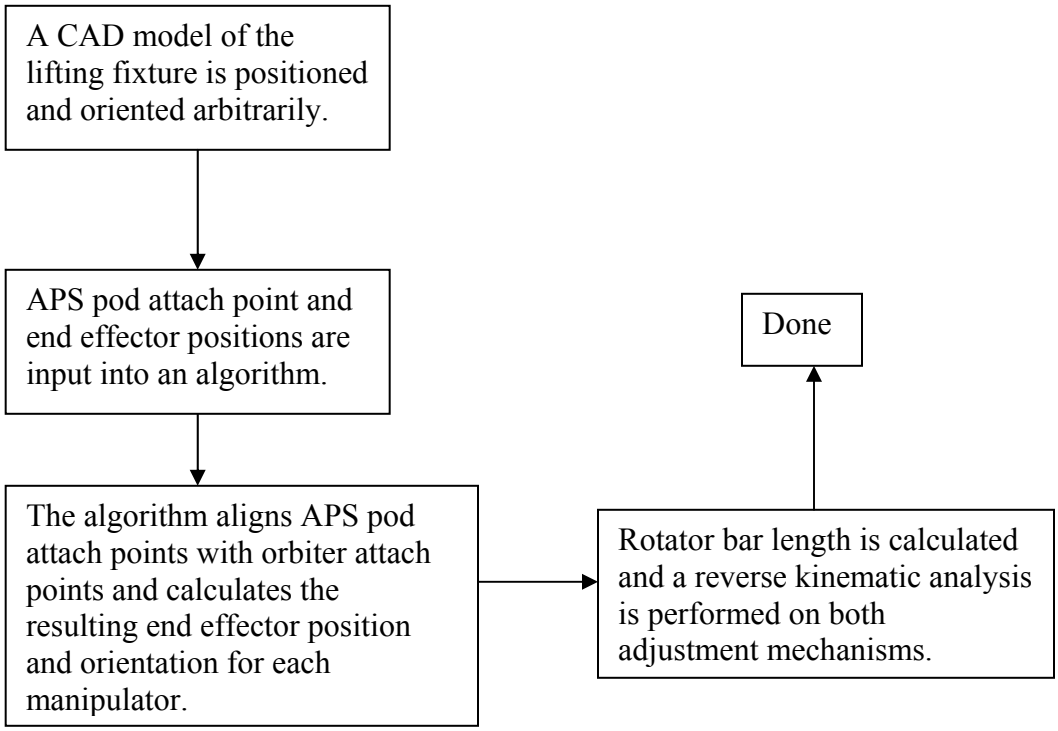

Figure 2-1 – Joint offset calculation procedure.

Determination of Desired Joint Angles

An existing Pro/E model of the lifting fixture, rotator bar, and adjustment mechanisms was refined for this analysis. The location of each end effector and APS pod attach point, in orbiter coordinates, was ascertained from the model and input into a C program. The C program translated and rotated the input points until the APS pod attach points were aligned with orbiter attach points. The resulting end effector points were used in reverse kinematic analyses to calculate joint angles. These joint angles can be described as the joint angles required to align the APS pod with the orbiter attach

points. The orbiter coordinate system and APS pod coordinate systems are discussed in detail in Appendix B.

Alignment of APS pod Attach Points with Orbiter Attach Points

The initial position and orientation of the lifting fixture in the CAD model is arbitrary. The lifting fixture's adjustments at attach points 1, 2, 3 and 4 have been physically measured and incorporated into the CAD model. The CAD model also contains seven points on the lifting fixture needed to describe end effector positions and orientations. Attach points 1, 2, and 3 are located in the CAD model of the left APS pod and their desired locations on the orbiter are also included in the model. Adjustment mechanism points can be seen below in Figure 2-2.

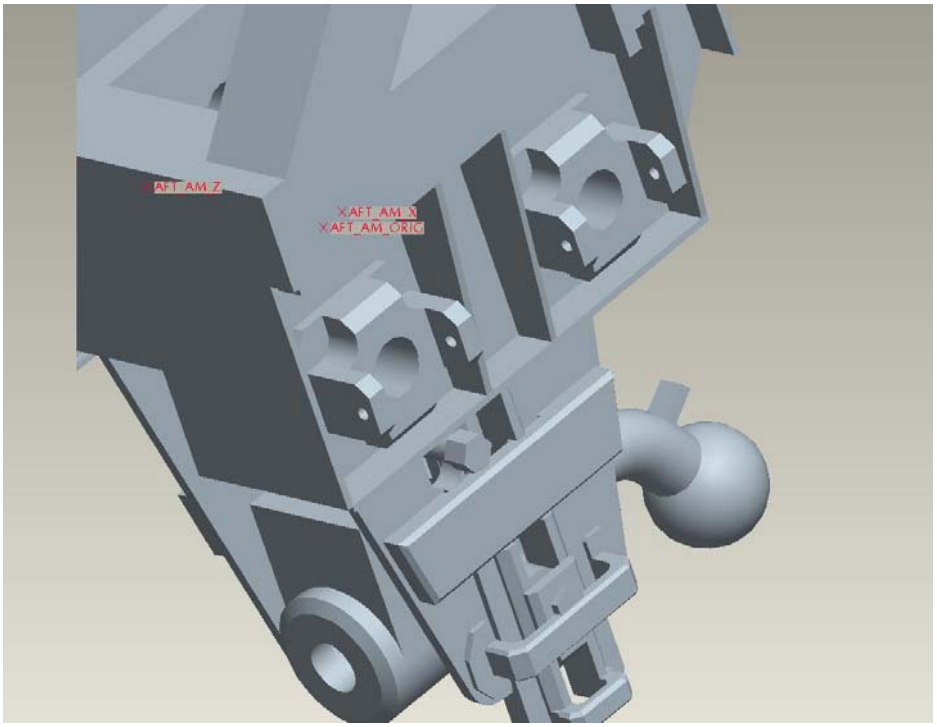

Figure 2-2 - Three points are needed to determine each adjustment mechanism's position and orientation (aft adjustment mechanism shown, typical of all adjustment mechanisms).

Attach point 3 has the most stringent accuracy requirements so it is aligned first. The alignment algorithm begins by calculating the misalignment of APS pod attach point 3, $\overrightarrow{P^{Pod}_{AttachPt3}}$, relative to orbiter attach point 3, $\overrightarrow{P^{Orbiter}_{AttachPt3}}$:

$$\overrightarrow{P_{Translate}} = \overrightarrow{P^{Orbiter}_{AttachPt3}} - \overrightarrow{P^{Pod}_{AttachPt3}} \tag{2.1}$$

The APS pod and lifting fixture can be translated such that APS pod attach point 3 is aligned by adding $\overrightarrow{P_{Translate}}$ to all points located on either object:

$$\begin{aligned}
\overrightarrow{P^{Pod}_{AttachPt1}} &= \overrightarrow{P^{Pod}_{AttachPt1}} + \overrightarrow{P_{Translate}} \\
\overrightarrow{P^{Pod}_{AttachPt2}} &= \overrightarrow{P^{Pod}_{AttachPt2}} + \overrightarrow{P_{Translate}} \\
\overrightarrow{P^{Pod}_{AttachPt3}} &= \overrightarrow{P^{Pod}_{AttachPt3}} + \overrightarrow{P_{Translate}} \\
\overrightarrow{P^{LiftingFixture}_{RotatorBar}} &= \overrightarrow{P^{LiftingFixture}_{RotatorBar}} + \overrightarrow{P_{Translate}} \\
\overrightarrow{P^{LiftingFixture}_{FwdAdjMechOrig}} &= \overrightarrow{P^{LiftingFixture}_{FwdAdjMechOrig}} + \overrightarrow{P_{Translate}} \\
\overrightarrow{P^{LiftingFixture}_{FwdAdjMechX}} &= \overrightarrow{P^{LiftingFixture}_{FwdAdjMechX}} + \overrightarrow{P_{Translate}} \\
\overrightarrow{P^{LiftingFixture}_{FwdAdjMechZ}} &= \overrightarrow{P^{LiftingFixture}_{FwdAdjMechZ}} + \overrightarrow{P_{Translate}} \\
\overrightarrow{P^{LiftingFixture}_{AftAdjMechOrig}} &= \overrightarrow{P^{LiftingFixture}_{AftAdjMechOrig}} + \overrightarrow{P_{Translate}} \\
\overrightarrow{P^{LiftingFixture}_{AftAdjMechX}} &= \overrightarrow{P^{LiftingFixture}_{AftAdjMechX}} + \overrightarrow{P_{Translate}} \\
\overrightarrow{P^{LiftingFixture}_{AftAdjMechZ}} &= \overrightarrow{P^{LiftingFixture}_{AftAdjMechZ}} + \overrightarrow{P_{Translate}}
\end{aligned} \tag{2.2}$$

Attach point 2 has the next most stringent accuracy requirements and therefore is aligned second. The unit vectors from pod attach point 3 to pod attach point 2 and pod attach point 3 to orbiter attach point 2 are described as:

$$\overrightarrow{V_{32\_Pod}} = \frac{\overrightarrow{P^{Pod}_{AttachPt2}} - \overrightarrow{P^{Pod}_{AttachPt3}}}{\left|\overrightarrow{P^{Pod}_{AttachPt2}} - \overrightarrow{P^{Pod}_{AttachPt3}}\right|}$$
$$\overrightarrow{V_{32\_Orb}} = \frac{\overrightarrow{P^{Orbiter}_{AttachPt2}} - \overrightarrow{P^{Pod}_{AttachPt3}}}{\left|\overrightarrow{P^{Orbiter}_{AttachPt2}} - \overrightarrow{P^{Pod}_{AttachPt3}}\right|} \tag{2.3}$$

The unit vector $\vec{m}_1$ perpendicular to both $\overrightarrow{V_{32\_Pod}}$ and $\overrightarrow{V_{32\_Orb}}$ can be calculated as

$$\vec{m}_1 = \frac{\overrightarrow{V_{32\_Pod}} \times \overrightarrow{V_{32\_Orb}}}{\left|\overrightarrow{V_{32\_Pod}} \times \overrightarrow{V_{32\_Orb}}\right|} \tag{2.4}$$

and the angle θ_2 between $\overrightarrow{V_{32\_Pod}}$ and $\overrightarrow{V_{32\_Orb}}$ is the unique solution to equations (2.5) and (2.6).

$$\theta_2 = \cos^{-1}\left(\overrightarrow{V_{32\_Pod}} \cdot \overrightarrow{V_{32\_Orb}}\right) \tag{2.5}$$

$$\theta_2 = \sin^{-1}\left|\overrightarrow{V_{32\_Pod}} \times \overrightarrow{V_{32\_Orb}}\right| \tag{2.6}$$

Pod attach point 2 will become aligned – and pod attach point 3 will remain aligned – if lifting fixture and APS pod points are rotated by angle θ_2 about an axis containing vector $\vec{m}_1$ and passing through pod attach point 3. This transformation matrix T_1 is calculated using an equation listed in [1]:

$$T_1 = \begin{bmatrix} m_{1x}m_{1x}\upsilon_1 + \cos\theta_2 & m_{1x}m_{1y}\upsilon_1 - m_{1z}\sin\theta_2 & m_{1x}m_{1z}\upsilon_1 + m_{1y}\sin\theta_2 & P^{Pod}_{AttachPt3,X} \\ m_{1x}m_{1y}\upsilon_1 + m_{1z}\sin\theta_2 & m_{1y}m_{1y}\upsilon_1 + \cos\theta_2 & m_{1y}m_{1z}\upsilon_1 - m_{1x}\sin\theta_2 & P^{Pod}_{AttachPt3,Y} \\ m_{1x}m_{1z}\upsilon_1 - m_{1y}\sin\theta_2 & m_{1y}m_{1z}\upsilon_1 + m_{1x}\sin\theta_2 & m_{1z}m_{1z}\upsilon_1 + \cos\theta_2 & P^{Pod}_{AttachPt3,Z} \\ 0 & 0 & 0 & 1 \end{bmatrix} \quad (2.7)$$

$$\upsilon_1 \equiv 1 - \cos\theta_2$$

This rotation is subsequently performed on all APS pod and lifting fixture points.

$$\begin{bmatrix} \overrightarrow{P^{Pod}_{AttachPt1}} \\ 1 \end{bmatrix} = T_1 \begin{bmatrix} \overrightarrow{P^{Pod}_{AttachPt1}} - \overrightarrow{P^{Pod}_{AttachPt3}} \\ 1 \end{bmatrix}$$

$$\begin{bmatrix} \overrightarrow{P^{Pod}_{AttachPt2}} \\ 1 \end{bmatrix} = T_1 \begin{bmatrix} \overrightarrow{P^{Pod}_{AttachPt2}} - \overrightarrow{P^{Pod}_{AttachPt3}} \\ 1 \end{bmatrix}$$

$$\begin{bmatrix} \overrightarrow{P^{Pod}_{AttachPt3}} \\ 1 \end{bmatrix} = T_1 \begin{bmatrix} \overrightarrow{P^{Pod}_{AttachPt3}} - \overrightarrow{P^{Pod}_{AttachPt3}} \\ 1 \end{bmatrix}$$

$$\begin{bmatrix} \overrightarrow{P^{LiftingFixture}_{RotatorBar}} \\ 1 \end{bmatrix} = T_1 \begin{bmatrix} \overrightarrow{P^{LiftingFixture}_{RotatorBar}} - \overrightarrow{P^{Pod}_{AttachPt3}} \\ 1 \end{bmatrix}$$

$$\begin{bmatrix} \overrightarrow{P^{LiftingFixture}_{FwdAdjMechOrig}} \\ 1 \end{bmatrix} = T_1 \begin{bmatrix} \overrightarrow{P^{LiftingFixture}_{FwdAdjMechOrig}} - \overrightarrow{P^{Pod}_{AttachPt3}} \\ 1 \end{bmatrix}$$

$$\begin{bmatrix} \overrightarrow{P^{LiftingFixture}_{FwdAdjMechX}} \\ 1 \end{bmatrix} = T_1 \begin{bmatrix} \overrightarrow{P^{LiftingFixture}_{FwdAdjMechX}} - \overrightarrow{P^{Pod}_{AttachPt3}} \\ 1 \end{bmatrix}$$

$$\begin{bmatrix} \overrightarrow{P^{LiftingFixture}_{FwdAdjMechZ}} \\ 1 \end{bmatrix} = T_1 \begin{bmatrix} \overrightarrow{P^{LiftingFixture}_{FwdAdjMechZ}} - \overrightarrow{P^{Pod}_{AttachPt3}} \\ 1 \end{bmatrix}$$

$$\begin{bmatrix} \overrightarrow{P^{LiftingFixture}_{AftAdjMechOrig}} \\ 1 \end{bmatrix} = T_1 \begin{bmatrix} \overrightarrow{P^{LiftingFixture}_{AftAdjMechOrig}} - \overrightarrow{P^{Pod}_{AttachPt3}} \\ 1 \end{bmatrix}$$

$$\begin{bmatrix} \overrightarrow{P^{LiftingFixture}_{AftAdjMechX}} \\ 1 \end{bmatrix} = T_1 \begin{bmatrix} \overrightarrow{P^{LiftingFixture}_{AftAdjMechX}} - \overrightarrow{P^{Pod}_{AttachPt3}} \\ 1 \end{bmatrix} \quad (2.8)$$

$$\begin{bmatrix} \overrightarrow{P^{LiftingFixture}_{AftAdjMechZ}} \\ 1 \end{bmatrix} = T_1 \begin{bmatrix} \overrightarrow{P^{LiftingFixture}_{AftAdjMechZ}} - \overrightarrow{P^{Pod}_{AttachPt3}} \\ 1 \end{bmatrix}$$

Another rotation must be performed to align pod attach point 1. The axis of rotation must pass through pod attach point 2 and pod attach point 3 so that these points do not become misaligned. The Plücker coordinates of this line are

$$\{\vec{S}_2;\vec{S}_{OL2}\} = \{\overrightarrow{V_{32\_Orb}};\overrightarrow{P^{Pod}_{AttachPt3}}\times\overrightarrow{V_{32\_Orb}}\} \tag{2.9}$$

and the parallel line passing through pod attach point 1 is given as

$$\{\vec{S}_1;\vec{S}_{OL1}\} = \{\overrightarrow{V_{32\_Orb}};\overrightarrow{P^{Pod}_{AttachPt1}}\times\overrightarrow{V_{32\_Orb}}\} \tag{2.10}$$

Vectors $\overrightarrow{p_1}$ and $\overrightarrow{p_2}$ are perpendicular to each line and originate at the orbiter coordinate system origin.

$$\begin{aligned}\overrightarrow{p_1} &= \vec{S}_1\times\overrightarrow{S_{OL1}}\\ \overrightarrow{p_2} &= \vec{S}_2\times\overrightarrow{S_{OL2}}\end{aligned} \tag{2.11}$$

When aligned, pod attach point 1 will reside on the y_{pod}=100 plane. The y_{pod} coordinate of pod attach point 1 can be calculated using part of the ${}^{LeftPod}_{Orbiter}T$ transformation matrix:

$$y_{pod} = \begin{bmatrix}-0.0526981625 & -0.7183402679 & 0.6936931332 & -194.96530381\end{bmatrix}\begin{bmatrix}\overrightarrow{P^{Pod}_{AttachPt1}}\\ 1\end{bmatrix} \tag{2.12}$$

The required angle of rotation θ_1 can now be calculated.

$$\theta_1 = \sin^{-1}\left(\frac{\mathrm{y_{pod}} - 100}{\left|\overrightarrow{p_2} - \overrightarrow{p_1}\right|}\right) \tag{2.13}$$

$$\theta_1 = \cos^{-1}\left(\frac{\sqrt{\left(\overrightarrow{p_2} - \overrightarrow{p_1}\right)^2 - \left(y_{pod} - 100\right)^2}}{\left|\overrightarrow{p_2} - \overrightarrow{p_1}\right|}\right) \tag{2.14}$$

The transformation matrix equation in [1] can be utilized again to calculate transformation matrix T_2.

$$T_2 = \begin{bmatrix} V_{32\_Pod,x}V_{32\_Pod,x}\upsilon_2 + \cos\theta_1 & V_{32\_Pod,x}V_{32\_Pod,y}\upsilon_2 - V_{32\_Pod,z}\sin\theta_1 & V_{32\_Pod,x}V_{32\_Pod,z}\upsilon_2 + V_{32\_Pod,y}\sin\theta_1 & P^{Pod}_{AttachPt3,x} \\ V_{32\_Pod,x}V_{32\_Pod,y}\upsilon_2 + V_{32\_Pod,z}\sin\theta_1 & V_{32\_Pod,y}V_{32\_Pod,y}\upsilon_2 + \cos\theta_1 & V_{32\_Pod,y}V_{32\_Pod,z}\upsilon_2 - V_{32\_Pod,x}\sin\theta_1 & P^{Pod}_{AttachPt3,y} \\ V_{32\_Pod,x}V_{32\_Pod,z}\upsilon_2 - V_{32\_Pod,y}\sin\theta_1 & V_{32\_Pod,y}V_{32\_Pod,z}\upsilon_2 + V_{32\_Pod,x}\sin\theta_1 & V_{32\_Pod,z}V_{32\_Pod,z}\upsilon_2 + \cos\theta_1 & P^{Pod}_{AttachPt3,z} \\ 0 & 0 & 0 & 1 \end{bmatrix} \tag{2.15}$$

where $\upsilon_2 \equiv 1 - \cos\theta_1$

Transformation matrix T_2 is then used to perform the rotation of all points about the line passing through pod attach point 2 and pod attach point 3.

$$
\begin{aligned}
\begin{bmatrix} \overrightarrow{P^{Pod}_{AttachPt1}} \\ 1 \end{bmatrix} &= T_2 \begin{bmatrix} \overrightarrow{P^{Pod}_{AttachPt1}} - \overrightarrow{P^{Pod}_{AttachPt3}} \\ 1 \end{bmatrix} \\
\begin{bmatrix} \overrightarrow{P^{Pod}_{AttachPt2}} \\ 1 \end{bmatrix} &= T_2 \begin{bmatrix} \overrightarrow{P^{Pod}_{AttachPt2}} - \overrightarrow{P^{Pod}_{AttachPt3}} \\ 1 \end{bmatrix} \\
\begin{bmatrix} \overrightarrow{P^{Pod}_{AttachPt3}} \\ 1 \end{bmatrix} &= T_2 \begin{bmatrix} \overrightarrow{P^{Pod}_{AttachPt3}} - \overrightarrow{P^{Pod}_{AttachPt3}} \\ 1 \end{bmatrix} \\
\begin{bmatrix} \overrightarrow{P^{LiftingFixture}_{RotatorBar}} \\ 1 \end{bmatrix} &= T_2 \begin{bmatrix} \overrightarrow{P^{LiftingFixture}_{RotatorBar}} - \overrightarrow{P^{Pod}_{AttachPt3}} \\ 1 \end{bmatrix} \\
\begin{bmatrix} \overrightarrow{P^{LiftingFixture}_{FwdAdjMechOrig}} \\ 1 \end{bmatrix} &= T_2 \begin{bmatrix} \overrightarrow{P^{LiftingFixture}_{FwdAdjMechOrig}} - \overrightarrow{P^{Pod}_{AttachPt3}} \\ 1 \end{bmatrix} \\
\begin{bmatrix} \overrightarrow{P^{LiftingFixture}_{FwdAdjMechX}} \\ 1 \end{bmatrix} &= T_2 \begin{bmatrix} \overrightarrow{P^{LiftingFixture}_{FwdAdjMechX}} - \overrightarrow{P^{Pod}_{AttachPt3}} \\ 1 \end{bmatrix} \\
\begin{bmatrix} \overrightarrow{P^{LiftingFixture}_{FwdAdjMechZ}} \\ 1 \end{bmatrix} &= T_2 \begin{bmatrix} \overrightarrow{P^{LiftingFixture}_{FwdAdjMechZ}} - \overrightarrow{P^{Pod}_{AttachPt3}} \\ 1 \end{bmatrix} \\
\begin{bmatrix} \overrightarrow{P^{LiftingFixture}_{AftAdjMechOrig}} \\ 1 \end{bmatrix} &= T_2 \begin{bmatrix} \overrightarrow{P^{LiftingFixture}_{AftAdjMechOrig}} - \overrightarrow{P^{Pod}_{AttachPt3}} \\ 1 \end{bmatrix} \\
\begin{bmatrix} \overrightarrow{P^{LiftingFixture}_{AftAdjMechX}} \\ 1 \end{bmatrix} &= T_2 \begin{bmatrix} \overrightarrow{P^{LiftingFixture}_{AftAdjMechX}} - \overrightarrow{P^{Pod}_{AttachPt3}} \\ 1 \end{bmatrix} \\
\begin{bmatrix} \overrightarrow{P^{LiftingFixture}_{AftAdjMechZ}} \\ 1 \end{bmatrix} &= T_2 \begin{bmatrix} \overrightarrow{P^{LiftingFixture}_{AftAdjMechZ}} - \overrightarrow{P^{Pod}_{AttachPt3}} \\ 1 \end{bmatrix}
\end{aligned}
\tag{2.16}
$$

APS pod attach points 1, 2, and 3 have been aligned. A reverse kinematic analysis will now be conducted to determine the adjustment mechanism joint angles with the APS pod aligned.

Adjustment Mechanism Reverse Kinematic Analysis

Adjustment Mechanism Parameters

Joint axis vectors $\overrightarrow{S_j}$ and link vectors $\overrightarrow{a_{ij}}$ must be chosen for the adjustment mechanisms. These selections are shown in Figure 2-3 below. It should be noted that the spherical joints are treated as "three noncoplanar cointersecting revolute joints" [1].

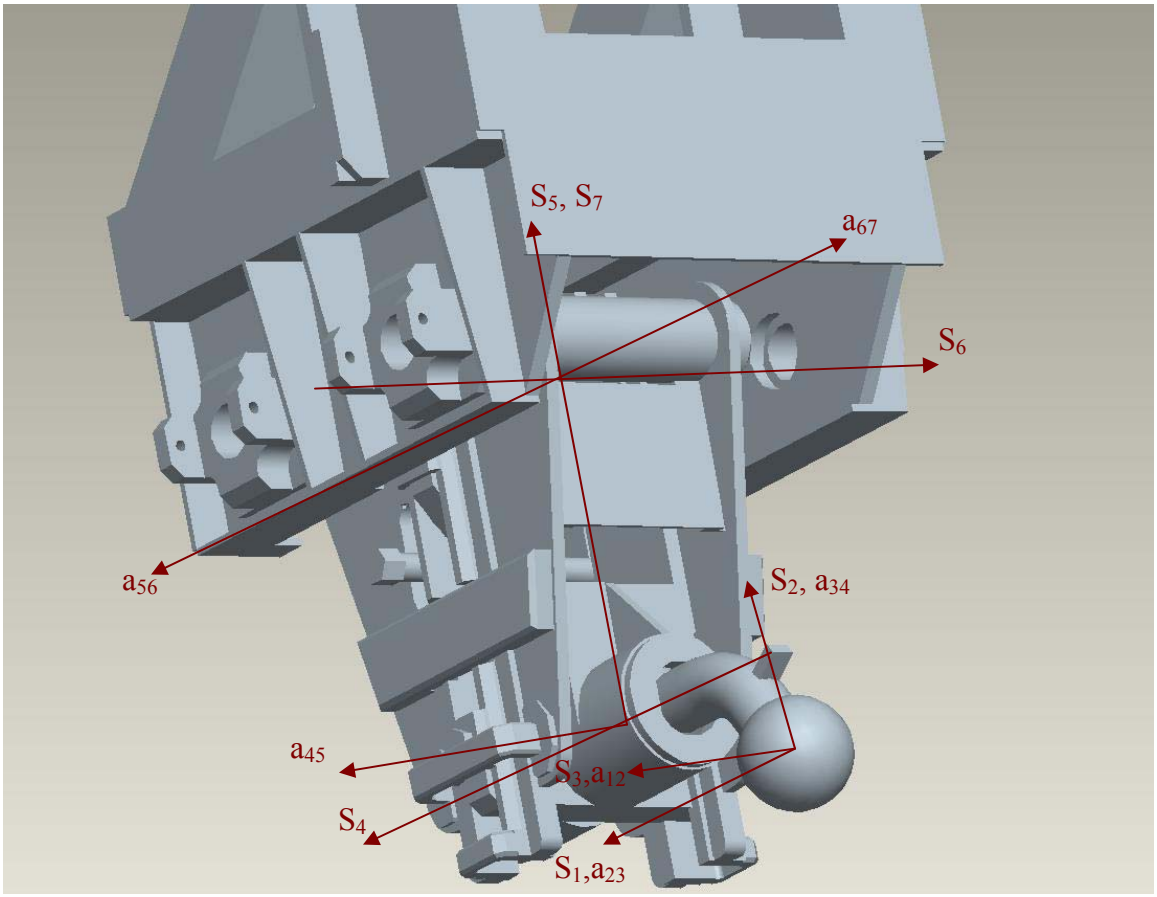

Figure 2-3 - Adjustment mechanism joint axis vectors and link vectors.

Joint angle θ_j is defined as the angle from $\overrightarrow{a_{ij}}$ to $\overrightarrow{a_{jk}}$ about the vector $\overrightarrow{S_j}$.

Similarly, twist angle α_{ij} is defined as the angle from $\overrightarrow{S_i}$ to $\overrightarrow{S_j}$ about the vector $\overrightarrow{a_{ij}}$.

$$\begin{aligned} \overrightarrow{S_j}\sin\theta_j &= \overrightarrow{a_{ij}} \times \overrightarrow{a_{jk}} \\ \overrightarrow{a_{ij}}\sin\alpha_{ij} &= \overrightarrow{S_i} \times \overrightarrow{S_j} \end{aligned} \tag{2.17}$$

Joint offset S_j is the distance from $\overrightarrow{a_{ij}}$ to $\overrightarrow{a_{jk}}$ along $\overrightarrow{S_j}$. Link length a_{ij} is the distance from $\overrightarrow{S_i}$ to $\overrightarrow{S_j}$ along $\overrightarrow{a_{ij}}$. The first joint angle, φ_1, describes the angle from fixed coordinate system X- axis and vector $\overrightarrow{a_{12}}$.

$$\overrightarrow{S_1}\sin\phi_1 = \overrightarrow{X_{Fixed}} \times \overrightarrow{a_{12}} \tag{2.18}$$

Adjustment mechanism joint angles, twist angles, joint offsets, and link lengths are defined in Table 2-1. The constant parameters are exactly the same for both forward and aft adjustment mechanisms. Parameters marked as 'variable' are not necessarily the same for both adjustment mechanisms because adjustment mechanism end effector positions are not identical. Close-the-loop variables are created by the hypothetical closure link described in [1]. a_{67} and α_{67} are user-specified values (rather than a function of manipulator geometry) since the seventh joint is hypothetical.

Link Length, inches	**Twist Angle, degrees**	**Joint Offset, inches**	**Joint Angle, degrees**
$a_{12} = 0.000$	$\alpha_{12} = 270.0$	S_1 = Close-the-loop variable	φ_1 = variable
$a_{23} = 0.000$	$\alpha_{23} = 270.0$	$S_2 = 0.000$	θ_2 = variable
$a_{34} = 4.147$	$\alpha_{34} = 270.0$	$S_3 = 0.000$	θ_3 = variable
$a_{45} = 0.000$	$\alpha_{45} = 270.0$	S_4 = variable	$\theta_4 = 270.0$
$a_{56} = 0.000$	$\alpha_{56} = 90.0$	S_5 = variable	$\theta_5 = 270.0$
$a_{67} = 0.000$	$\alpha_{67} = 90.0$	S_6 = variable	$\theta_6 = 180.0$
a_{71} = Close-the-loop variable	α_{71} = Close-the-loop variable	S_7 = Close-the-loop variable	θ_7 = Close-the-loop variable

Table 2-1 - Adjustment mechanism parameters.

Close-the-Loop Variable Calculations

Close-the-loop variables can be calculated using the constant mechanism parameters listed in Table 2-1. ${}^{Fixed}\overrightarrow{S_1}$ is defined as $\begin{bmatrix}0 & 0 & 1\end{bmatrix}^T$ since the vector $\overrightarrow{S_1}$ is

exactly aligned with the fixed coordinate system Z- axis. ${}^{Fixed}\overrightarrow{S_7}$ is given by the expression

$${}^{Fixed}\overrightarrow{S_7} = {}^{Fixed}\overrightarrow{a_{67}} \times {}^{Fixed}\overrightarrow{S_6} \tag{2.19}$$

Unit vectors ${}^{Fixed}\overrightarrow{a_{67}}$ and ${}^{Fixed}\overrightarrow{S_6}$ are the X- axis and Z- axis of the adjustment mechanism 6th coordinate system, respectively. They can be calculated as

$$\begin{aligned} {}^{Fixed}\overrightarrow{a_{67}} &= \overrightarrow{P^{LiftingFixture}_{FwdAdjMechX}} - \overrightarrow{P^{LiftingFixture}_{AdjMechOrig}} \\ {}^{Fixed}\overrightarrow{S_6} &= \overrightarrow{P^{LiftingFixture}_{FwdAdjMechZ}} - \overrightarrow{P^{LiftingFixture}_{AdjMechOrig}} \end{aligned} \tag{2.20}$$

These definitions allow the unit vector ${}^{Fixed}\overrightarrow{a71}$ to be determined from

$${}^{Fixed}\overrightarrow{a_{71}} = \frac{{}^{Fixed}\overrightarrow{S_7} \times {}^{Fixed}\overrightarrow{S_1}}{\left| {}^{Fixed}\overrightarrow{S_7} \times {}^{Fixed}\overrightarrow{S_1} \right|} \tag{2.21}$$

The close-the-loop variables can now be calculated. A unique value for the twist angle α_{71} between vectors $\overrightarrow{S_7}$ and $\overrightarrow{S_1}$ is given by

$$\begin{aligned} \cos(\alpha_{71}) &= {}^{Fixed}\overrightarrow{S_7} \cdot {}^{Fixed}\overrightarrow{S_1} \\ \sin(\alpha_{71}) &= \left({}^{Fixed}\overrightarrow{S_7} \times {}^{Fixed}\overrightarrow{S_1} \right) \cdot {}^{Fixed}\overrightarrow{a_{71}} \end{aligned} \tag{2.22}$$

Similarly, the joint angle θ_7 can be found

$$\begin{aligned} \cos(\theta_7) &= {}^{Fixed}\overrightarrow{a_{67}} \cdot {}^{Fixed}\overrightarrow{a_{71}} \\ \sin(\theta_7) &= \left({}^{Fixed}\overrightarrow{a_{67}} \times {}^{Fixed}\overrightarrow{a_{71}} \right) \cdot {}^{Fixed}\overrightarrow{S_7} \end{aligned} \tag{2.23}$$

The angle γ_1 is defined as the angle between $\overrightarrow{a_{71}}$ and the X- axis of the fixed coordinate system.

$$\begin{aligned} \cos(\gamma_1) &= {}^{Fixed}\overrightarrow{a_{71}} \cdot \begin{bmatrix} 1 & 0 & 0 \end{bmatrix}^T \\ \sin(\gamma_1) &= \left({}^{Fixed}\overrightarrow{a_{71}} \times \begin{bmatrix} 1 & 0 & 0 \end{bmatrix}^T \right) \cdot {}^{Fixed}\overrightarrow{S_1} \end{aligned} \tag{2.24}$$

The joint offset S_7 along the $\overrightarrow{S_7}$ vector can be calculated by

$$S_7 = \frac{\left({}^{Fixed}\overrightarrow{S_1} \times \overrightarrow{P^{LiftingFixture}_{AdjMechOrig}} \right) \cdot {}^{Fixed}\overrightarrow{a_{71}}}{\sin(\alpha_{71})} \tag{2.25}$$

The link length a_{71} along the $\overrightarrow{a_{71}}$ vector is given by

$$a_{71} = \frac{\left(\overrightarrow{P^{LiftingFixture}_{AdjMechOrig}} \times {}^{Fixed}\overrightarrow{S_1} \right) \cdot {}^{Fixed}\overrightarrow{S_7}}{\sin(\alpha_{71})} \tag{2.26}$$

Joint offset S_1 along the $\overrightarrow{S_1}$ vector is

$$S_1 = \frac{\left(\overrightarrow{P^{LiftingFixture}_{AdjMechOrig}} \times {}^{Fixed}\overrightarrow{S_7} \right) \cdot {}^{Fixed}\overrightarrow{a_{71}}}{\sin(\alpha_{71})} \tag{2.27}$$

The close-the-loop variables α_{71}, θ_7, γ_1, S_7, a_{71}, and S_1 will be used in the reverse kinematic analysis of this PPPS mechanism.

PPPS Reverse Kinematic Analysis

As previously stated, the adjustment mechanisms are RPPPS spatial mechanisms but will be analyzed as an equivalent RPPPRRR mechanism. They are categorized as group 1 mechanisms since the spatial mechanisms and equivalent spherical mechanisms have a single degree-of-freedom.

Spherical equations generally contain a high number of terms. However, these terms exist in patterns that allow a short-hand notation to describe the equation more concisely. Notation variables are defined in Appendix C.

θ_1 is the first unknown joint angle that will be calculated. The fundamental spherical heptagon equation

$$Z_{45671} = c_{23} \tag{2.28}$$

can be expanded to

$$s_{12}\left(X_{4567}s_1 + Y_{4567}c_1\right) + c_{12}Z_{4567} = c_{23} \tag{2.29}$$

X_{4567} and Y_{4567} are defined by notation variables X_{456} and Y_{456}

$$\begin{aligned} \mathrm{X}_{4567} &\equiv \mathrm{X}_{456}c_7 - Y_{456}s_7 \\ Y_{4567} &\equiv c_{71}\left(\mathrm{X}_{456}s_7 + \mathrm{Y}_{456}c_7\right) - s_{71}\mathrm{Z}_{456} \\ Z_{4567} &\equiv s_{71}\left(\mathrm{X}_{456}s_7 + \mathrm{Y}_{456}c_7\right) + c_{71}\mathrm{Z}_{456} \end{aligned} \tag{2.30}$$

θ_7 and α_{71} are close-the-loop variables that have already been calculated, so X_{456}, Y_{456}, and Z_{456} are the only unknown terms that must be calculated. They can be defined as

$$\begin{aligned} \mathrm{X}_{456} &\equiv \mathrm{X}_{45}c_6 - Y_{45}s_6 \\ Y_{456} &\equiv c_{67}\left(\mathrm{X}_{45}s_6 + \mathrm{Y}_{45}c_6\right) - s_{67}\mathrm{Z}_{45} \\ Z_{456} &\equiv s_{67}\left(X_{45}s_6 + Y_{45}c_6\right) + c_{67}\mathrm{Z}_{45} \end{aligned} \tag{2.31}$$

θ_6 is a constant mechanism parameter and α_{67} is a user-specified value, so both are known quantities. X_{45}, Y_{45}, and Z_{45} must now be defined.

$$\begin{aligned} \mathrm{X}_{45} &\equiv \mathrm{X}_4c_5 - Y_4s_5 \\ Y_{45} &\equiv c_{56}\left(\mathrm{X}_4s_5 + \mathrm{Y}_4c_5\right) - s_{56}\mathrm{Z}_4 \\ Z_{45} &\equiv s_{56}\left(X_4s_5 + Y_4c_5\right) + c_{56}\mathrm{Z}_4 \end{aligned} \tag{2.32}$$

θ_5 and α_{56} are constant mechanism parameters. X_4, Y_4, and Z_4 are defined as

$$\begin{aligned} \mathrm{X}_4 &\equiv s_{34}s_4 \\ Y_4 &\equiv -\left(\mathrm{s}_{45}c_{34} + \mathrm{c}_{45}s_{34}c_4\right) \\ Z_4 &\equiv c_{45}c_{34} - \mathrm{s}_{45}s_{34}c_4 \end{aligned} \tag{2.33}$$

θ_4, α_{34} and α_{45} are constant mechanism parameters so X_4, Y_4, and Z_4 can be calculated. Using substitution, X_{4567} and Y_{4567} can now be calculated. This results in an equation of the form $Ac_1 + Bs_1 + D = 0$. Using the trigonometric solution method described in [1], θ_1 can be calculated

$$\theta_1 = \cos^{-1}\left(\frac{c_{23} - c_{12}Z_{4567}}{\sqrt{\left(\mathrm{s}_{12}\mathrm{Y}_{4567}\right)^2 + \left(\mathrm{s}_{12}X_{4567}\right)^2}}\right) + \gamma \tag{2.34}$$

where γ is the unique solution of

$$\begin{aligned}\gamma &= \sin^{-1}\left(\frac{\mathrm{s}_{12}\mathrm{X}_{4567}}{\sqrt{\left(\mathrm{s}_{12}\mathrm{Y}_{4567}\right)^2 + \left(\mathrm{s}_{12}\mathrm{X}_{4567}\right)^2}}\right)\\ \gamma &= \cos^{-1}\left(\frac{\mathrm{s}_{12}\mathrm{Y}_{4567}}{\sqrt{\left(\mathrm{s}_{12}\mathrm{Y}_{4567}\right)^2 + \left(\mathrm{s}_{12}\mathrm{X}_{4567}\right)^2}}\right)\end{aligned} \tag{2.35}$$

It should be noted that θ_1 has two solutions, designated as θ_{1A} and θ_{1B}. Other joint angles are a function of θ_1, so it is necessary to solve each joint angle using θ_{1A} and θ_{1B}. There are two sets of joint angles, solution set A and solution set B, that satisfy the input end effector position and orientation for the specified manipulator geometry.

Unknown joint angle θ_2 can now be calculated using θ_{1A} and θ_{1B}. The fundamental spherical heptagon equations

$$\begin{aligned}X_{45671} &= s_{23}s_2\\ Y_{45671} &= s_{23}c_2\end{aligned} \tag{2.36}$$

will be used. Since X_{4567}, Y_{4567}, and Z_{4567} were determined in the θ_1 derivation, X_{45671} and Y_{45671} can be calculated immediately using θ_{1A} and θ_{1B}.

$$\begin{aligned}X_{45671} &\equiv X_{4567}c_1 - Y_{4567}s_1\\ Y_{45671} &\equiv c_{12}\left(\mathrm{X}_{4567}s_1 + \mathrm{Y}_{4567}c_1\right) - \mathrm{s}_{12}\mathrm{Z}_{4567}\end{aligned} \tag{2.37}$$

θ_2 is the unique solution to

$$\begin{aligned}\theta_2 &= \sin^{-1}\left(\frac{X_{45671}}{s_{23}}\right)\\ \theta_2 &= \cos^{-1}\left(\frac{Y_{45671}}{s_{23}}\right)\end{aligned} \tag{2.38}$$

for the solution set containing θ_{1A} and the set containing θ_{1B}.

The reverse kinematic analysis continues with the calculation of unknown joint angle θ_3. The fundamental spherical heptagon equations

$$\begin{aligned} X_{56712} &= s_{34}s_3 \\ Y_{56712} &= s_{34}c_3 \end{aligned} \tag{2.39}$$

can be used because θ_{1A}, θ_{1B}, θ_{2A} and θ_{2B} have been calculated. X_{56712} and Y_{56712} are defined as

$$\begin{aligned} X_{56712} &\equiv X_{5671}c_2 - Y_{5671}s_2 \\ Y_{56712} &\equiv c_{23}\left(\mathrm{X}_{5671}s_2 + \mathrm{Y}_{5671}c_2\right) - \mathrm{s}_{23}\mathrm{Z}_{5671} \end{aligned} \tag{2.40}$$

Similar to the solution for θ_1, the solution for θ_3 proceeds by solving for the notation variables that comprise X_{56712} and Y_{56712}.

$$\begin{aligned} \mathrm{X}_{5671} &\equiv \mathrm{X}_{567}c_1 - Y_{567}s_1 \\ Y_{5671} &\equiv c_{12}\left(\mathrm{X}_{567}s_1 + \mathrm{Y}_{567}c_1\right) - s_{12}\mathrm{Z}_{567} \\ Z_{5671} &\equiv s_{12}\left(\mathrm{X}_{567}s_1 + \mathrm{Y}_{567}c_1\right) + c_{12}\mathrm{Z}_{567} \end{aligned}$$

$$\begin{aligned} \mathrm{X}_{567} &\equiv \mathrm{X}_{56}c_6 - Y_{56}s_6 \\ Y_{567} &\equiv c_{71}\left(\mathrm{X}_{56}s_7 + \mathrm{Y}_{56}c_7\right) - s_{71}\mathrm{Z}_{56} \\ Z_{567} &\equiv s_{71}\left(X_{56}s_7 + Y_{56}c_7\right) + c_{71}\mathrm{Z}_{56} \end{aligned}$$

$$\begin{aligned} \mathrm{X}_{56} &\equiv \mathrm{X}_5c_6 - Y_5s_6 \\ Y_{56} &\equiv c_{67}\left(\mathrm{X}_5s_6 + \mathrm{Y}_5c_6\right) - s_{67}\mathrm{Z}_5 \\ Z_{56} &\equiv s_{67}\left(X_5s_6 + Y_5c_6\right) + c_{67}\mathrm{Z}_5 \end{aligned}$$

$$\begin{aligned} \mathrm{X}_5 &\equiv s_{45}s_5 \\ Y_5 &\equiv -\left(\mathrm{s}_{56}c_{45} + \mathrm{c}_{56}s_{45}c_5\right) \\ Z_5 &\equiv c_{56}c_{45} - \mathrm{s}_{56}s_{45}c_5 \end{aligned} \tag{2.41}$$

A unique solution for joint angle θ_3 can now be calculated for solution set A and solution set B using their associated joint angles.

$$\theta_3 = \sin^{-1}\left(\frac{X_{56712}}{s_{34}}\right)$$
$$\theta_3 = \cos^{-1}\left(\frac{Y_{56712}}{s_{34}}\right) \tag{2.42}$$

Joint offset S_4 will be calculated using the vector loop equation. The vector loop equation is given by

$$S_1\overrightarrow{S_1} + a_{12}\overrightarrow{a_{12}} + S_2\overrightarrow{S_2} + a_{23}\overrightarrow{a_{23}} + S_3\overrightarrow{S_3} + a_{34}\overrightarrow{a_{34}} + S_4\overrightarrow{S_4} + a_{45}\overrightarrow{a_{45}} + S_5\overrightarrow{S_5} + a_{56}\overrightarrow{a_{56}} + S_6\overrightarrow{S_6} + a_{67}\overrightarrow{a_{67}} + S_7\overrightarrow{S_7} + a_{71}\overrightarrow{a_{71}} = \vec{0} \tag{2.43}$$

Since several of these offsets are zero, the vector loop equation can be reduced to

$$S_1\overrightarrow{S_1} + a_{34}\overrightarrow{a_{34}} + S_4\overrightarrow{S_4} + a_{67}\overrightarrow{a_{67}} + S_7\overrightarrow{S_7} + a_{71}\overrightarrow{a_{71}} = 0 \tag{2.44}$$

Using spatial heptagon direction cosines set 5 in [1], the vector loop equation becomes

$$S_1X_{76} + a_{34}W_{45} + S_4X_5 + a_{67}c_6 + S_7\overline{X_6} + a_{71}W_{76} = 0 \tag{2.45}$$

Several notation terms in equation (2.45) must be calculated

$$\begin{aligned}
X_{76} &\equiv \overline{X_7}c_6 - \overline{Y_7}s_6 \\
W_{45} &\equiv c_5c_4 - s_5s_4c_{45} \\
W_{76} &\equiv c_6c_7 - s_6s_7c_{67} \\
\overline{X_6} &\equiv s_{67}s_6 \\
\overline{X_7} &\equiv s_{71}s_7 \\
\overline{Y_7} &\equiv -\left(s_{67}c_{71} + c_{67}s_{71}c_7\right)
\end{aligned} \tag{2.46}$$

Unknown joint offset S_4 can now be calculated by solving equation (2.45) for S_4.

$$S_4 = \frac{-S_1X_{76} - a_{34}W_{45} - a_{67}c_6 - S_7\overline{X_6} - a_{71}W_{76}}{X_5} \tag{2.47}$$

Joint offset S_6 is calculated by substituting spatial heptagon direction cosines set 4 into the vector loop equation. Equation (2.44) then reduces to

$$S_1 X_{765} + a_{34} c_4 + S_6 \overline{X_5} + a_{67} W_{65} + S_7 X_{65} + a_{71} W_{765} = 0 \tag{2.48}$$

Equation (2.48) can be further reduced by noting that c_4=0.

$$S_1 X_{765} + S_6 \overline{X_5} + a_{67} W_{65} + S_7 X_{65} + a_{71} W_{765} = 0 \tag{2.49}$$

The unknown notation variables can be calculated from

$$\begin{aligned}
&\mathrm{X}_{765} \equiv X_{76} c_5 - Y_{76} s_5 \\
&Y_{76} \equiv c_{56} \left(\overline{X_7} s_6 + \overline{Y_7} c_6 \right) - s_{56} \overline{Z_7} \\
&\overline{\mathrm{Z}_7} \equiv c_{67} c_{71} - s_{71} c_7 \\
&\overline{\mathrm{X}_5} \equiv s_{56} s_5 \\
&\mathrm{X}_{65} \equiv \overline{X_6} c_5 - \overline{Y_6} s_5 \\
&\overline{Y_6} = -\left(s_{56} c_{67} + c_{56} s_{67} c_6 \right) \\
&W_{65} \equiv c_5 c_6 - s_5 s_6 c_{56} \\
&\mathrm{W}_{765} \equiv s_5 \left(U_{76} s_{56} + V_{76} c_{56} \right) + c_5 W_{76} \\
&U_{76} \equiv s_7 s_{67} \\
&V_{76} \equiv -\left(s_6 c_7 + c_6 s_7 c_{67} \right)
\end{aligned} \tag{2.50}$$

Solving equation (2.49) for S_6 yields

$$S_6 = \frac{-S_1 X_{765} - a_{67} W_{65} - S_7 X_{65} - a_{71} W_{765}}{\overline{X_5}} \tag{2.51}$$

The only joint offset that has not yet been calculated is S_5. Spatial heptagon direction cosines set 3 are substituted into the vector loop equation given in equation (2.44).

$$S_1 X_{23} + a_{34} + S_5 \overline{X_4} + a_{67} W_{654} + S_7 X_{654} + a_{71} W_{123} = 0 \tag{2.52}$$

Once again, notation variables must be calculated before the unknown joint offset can be determined.

$$
\begin{aligned}
&\mathrm{X}_{23} \equiv X_2 c_3 - Y_2 s_3 \\
&\mathrm{X}_2 \equiv s_{12} s_2 \\
&\mathrm{Y}_2 \equiv -\left(s_{12} c_{12} + c_{12} s_{12} c_2\right) \\
&\overline{\mathrm{X}_4} \equiv s_{45} s_4 \\
&X_{54} \equiv \overline{X_5} c_4 - \overline{Y_5} s_4 \\
&X_{654} \equiv X_{65} c_4 - Y_{65} s_4 \\
&\mathrm{Y}_{65} \equiv c_{45}\left(\overline{X_6} s_5 + \overline{Y_6} c_5\right) - s_{45} \overline{Z_6} \\
&\overline{\mathrm{Z}_6} \equiv c_{56} c_{67} - s_{56} s_{67} c_6 \\
&\mathrm{W}_{123} \equiv s_3\left(U_{12} s_{23} + V_{12} c_{23}\right) + c_3 W_{12} \\
&\mathrm{U}_{12} \equiv s_1 s_{12} \\
&V_{12} \equiv -\left(s_2 c_1 + c_2 s_1 c_{12}\right) \\
&W_{12} \equiv c_2 c_1 - s_2 s_1 c_{12}
\end{aligned}
\tag{2.53}
$$

Finally, joint offset S_5 can be calculated

$$
S_5 = \frac{-S_1 X_{23} - a_{34} - S_6 X_{54} - S_7 X_{654} - a_{71} W_{123}}{\overline{X_4}} \tag{2.54}
$$

Both solution sets have now been calculated. In the case of the adjustment mechanism, all three joint offsets are the same in both solution sets. These joint offsets will be used to orient the lifting fixture so that a finite element analysis can be performed.

Rotator Bar Length Calculation

The rotator bar can be described as a RRRCRR mechanism. A reverse kinematic analysis could be conducted to ascertain joint angles and joint offsets that result in the APS pod being aligned. In order to conduct this analysis, the position and orientation of the end effector relative to the base must be input. The position of the rotator bar 6th coordinate system origin has been previously defined as $\overrightarrow{P_{RotatorBar}^{LiftingFixture}}$. The orientation of the end effector can be determined by also inputting points on the $\overrightarrow{a_{67}}$ and $\overrightarrow{S_6}$ axes and subtracting $\overrightarrow{P_{RotatorBar}^{LiftingFixture}}$ from each to determine the unit vectors $\overrightarrow{a_{67}}$ and $\overrightarrow{S_6}$.

Prior to conducting a reverse kinematic analysis of the rotator bar, it was noted that unique geometry makes it possible to calculate the joint offset of the cylinder joint. With the exception of the cylinder joint offset, all rotator bar link lengths and joint offsets are zero. As a result, the cylinder joint offset can be calculated using the distance equation

$$S_3 = \sqrt{\begin{matrix}\left(P^{LiftingFixture}_{RotatorBarX} - P^{LiftingFixture}_{RotatorBarBaseX}\right)^2 + \left(P^{LiftingFixture}_{RotatorBarY} - P^{LiftingFixture}_{RotatorBarBaseY}\right)^2 \\ + \left(P^{LiftingFixture}_{RotatorBarZ} - P^{LiftingFixture}_{RotatorBarBaseZ}\right)^2\end{matrix}} \tag{2.55}$$

Although unknown joint angles could be calculated using S_3, they are not needed for this analysis.

Nominal Solution

A program was written to perform pod alignment and subsequent joint offset calculations as described in this chapter. The mechanism parameters specified in Table 2-1 and the input coordinates of points $\overrightarrow{P^{Pod}_{AttachPt1}}$, $\overrightarrow{P^{Pod}_{AttachPt2}}$, $\overrightarrow{P^{Pod}_{AttachPt3}}$, $\overrightarrow{P^{LiftingFixture}_{RotatorBar}}$, $\overrightarrow{P^{LiftingFixture}_{FwdAdjMechOrig}}$, $\overrightarrow{P^{LiftingFixture}_{FwdAdjMechX}}$, $\overrightarrow{P^{LiftingFixture}_{FwdAdjMechZ}}$, $\overrightarrow{P^{LiftingFixture}_{AftAdjMechOrig}}$, $\overrightarrow{P^{LiftingFixture}_{AftAdjMechX}}$, and $\overrightarrow{P^{LiftingFixture}_{AftAdjMechZ}}$ were used.

Table 2-2 compares the joint offsets calculated by the program to the joint offsets measured using a perfectly aligned APS pod CAD model. The similar results show that the program is able to accurately calculate joint offsets for a known lifting fixture location. The two solutions, solution A and solution B, have nearly identical joint offsets but differing joint angles (not shown).

	Forward Adjustment Mechanism			Aft Adjustment Mechanism			Rotator Bar
Measurement Method	**S_4**	**S_5**	**S_6**	**S_4**	**S_5**	**S_6**	**S_3**
CAD model	13.6655”	14.5243”	8.7968”	12.3174”	14.8512”	8.8823”	94.5707”
Program Solution A	13.6655”	14.5244”	8.7968”	12.3174”	14.8512”	8.8824”	94.5706”
Program Solution B	13.6655”	14.5243”	8.7968”	12.3174”	14.8512”	8.8824”	

Table 2-2 - Comparison of joint offsets calculated by the program to measured using the CAD model.

The program is also able to perform a reverse kinematic analysis for right APS pods. This is accomplished by inverting the sign of the input $Y_{orbiter}$ coordinates then proceeding with the rest of the solution method. Right APS pods, lifting fixtures and orbiter attach points are mirror images of left APS pods, lifting fixtures, and orbiter deck attach points.

CHAPTER 3
UNCERTAINTY ANALYSIS

Due to the stringent accuracy requirements associated with the APS pod installation operation, an uncertainty analysis was conducted to assess the validity of the proposed solution method. Two different uncertainty calculation methods were used to create an upper and lower bound for total uncertainty. The 100% covariance method produces very conservative results since it assumes all errors are at their maximum value. The root sum squared method provides more optimistic results. The 100% covariance and root

sum squared uncertainty calculations provide an upper and lower bound respectively for the total error that can be reasonably expected.

Off-Nominal Conditions Within Tolerance

Manufacturing tolerances can have a significant effect on the overall accuracy of a manipulator. As a result, precision manipulators are often manufactured with very tight tolerances.

Adjustment Mechanism Spherical Joint Socket Locations

There are manufacturing tolerances associated with the spherical joint sockets and the position of their mounting holes on the orbiter. These tolerances yield an uncertainty of ±0.0349" in the position of each spherical joint (both $X_{orbiter}$ and $Z_{orbiter}$ directions). The resulting misalignment of the APS pod can be seen in Tables 3-1 and 3-2 below.

Attach Point	Coordinate Axis	Nominal Solution	Fwd Socket Misaligned by 0.0349" in the $+X_{orbiter}$ and $+Z_{orbiter}$ Directions	Resulting Attach Point Misalignment
Attach Point 1	X_{pod}	106.5000"	106.4997"	0.0003"
	Y_{pod}	100.0000"	99.9992"	0.0008"
	Z_{pod}	152.3460"	152.3565"	-0.0105"
Attach Point 2	X_{pod}	106.5000"	106.5002"	-0.0002"
	Y_{pod}	100.0000"	99.9995"	0.0005"
	Z_{pod}	49.1790"	49.1895"	-0.0105"
Attach Point 3	X_{pod}	253.5000"	253.5002"	-0.0002"
	Y_{pod}	100.0000"	99.9992"	0.0008"
	Z_{pod}	39.7680"	39.7792"	-0.0112"

Table 3-1 - Uncertainty due to tolerances associated with the position of the forward spherical joint socket.

Attach Point	Coordinate Axis	Nominal Solution	Aft Socket Misaligned by 0.0349" in the $+X_{orbiter}$ and $+Z_{orbiter}$ Directions	Resulting Attach Point Misalignment
Attach Point 1	X_{pod}	106.5000"	106.4997"	0.0003"
	Y_{pod}	100.0000"	99.9992"	0.0008"
	Z_{pod}	152.3460"	152.3565"	0.0105"
Attach Point 2	X_{pod}	106.5000"	106.5002"	-0.0002"

	Y_{pod}	100.0000”	99.9995”	0.0005”
	Z_{pod}	49.1790”	49.1895”	-0.0105”
Attach Point 3	X_{pod}	253.5000”	253.5002”	-0.0002”
	Y_{pod}	100.0000”	99.9992”	0.0008”
	Z_{pod}	39.7680”	39.7792”	-0.0112”

Table 3-2 - Uncertainty due to tolerances associated with the position of the aft spherical joint socket.

Orbiter Attach Point Locations

There is also uncertainty associated with the position of the orbiter attach points on the orbiter. According to drawing tolerances, the orbiter attach points are located within 0.010” of their intended position in the X_{pod}, Y_{pod}, and Z_{pod} directions. The effect of a 0.0104” attach point misalignment in all directions on the alignment of an APS pod can be seen for each attach point individually in Tables 3-3, 3-4, and 3-5.

Attach Point	Coordinate Axis	Nominal Solution	Attach Point 1 Misalignment of 0.0104” in all three directions	Resulting Attach Point Misalignment
Attach Point 1	X_{pod}	106.5000”	106.5104”	-0.0104”
	Y_{pod}	100.0000”	100.0104”	-0.0104”
	Z_{pod}	152.3460”	152.3564”	-0.0104”
Attach Point 2	X_{pod}	106.5000”	106.5000”	0.0000”
	Y_{pod}	100.0000”	100.0000”	0.0000”
	Z_{pod}	49.1790”	49.1790”	0.0000”
Attach Point 3	X_{pod}	253.5000”	253.5000”	0.0000”
	Y_{pod}	100.0000”	100.0000”	0.0000”
	Z_{pod}	39.7680”	39.7680”	0.0000”

Table 3-3 - Uncertainty due to the tolerances associated with the attach point 1 location on the orbiter.

Attach Point	Coordinate Axis	Nominal Solution	Attach Point 2 Misalignment of 0.0104” in all three directions	Resulting Attach Point Misalignment
Attach Point 1	X_{pod}	106.5000”	106.5000”	0.0000”
	Y_{pod}	100.0000”	100.0000”	0.0000”
	Z_{pod}	152.3460”	152.3460”	0.0000”
Attach Point 2	X_{pod}	106.5000”	106.5104”	-0.0104”
	Y_{pod}	100.0000”	100.0104”	-0.0104”
	Z_{pod}	49.1790”	49.1894”	-0.0104”

Attach Point 3	$\mathbf{X_{pod}}$	253.5000”	253.5000”	0.0000”
	$\mathbf{Y_{pod}}$	100.0000”	100.0000”	0.0000”
	$\mathbf{Z_{pod}}$	39.7680”	39.7680”	0.0000”

Table 3-4 - Uncertainty due to the tolerances associated with the attach point 2 location on the orbiter.

Attach Point	Coordinate Axis	Nominal Solution	Attach Point 3 Misalignment of 0.0104” in all three directions	Resulting Attach Point Misalignment
Attach Point 1	$\mathbf{X_{pod}}$	106.5000”	106.5000”	0.0000”
	$\mathbf{Y_{pod}}$	100.0000”	100.0000”	0.0000”
	$\mathbf{Z_{pod}}$	152.3460”	152.3460”	0.0000”
Attach Point 2	$\mathbf{X_{pod}}$	106.5000”	106.5000”	0.0000”
	$\mathbf{Y_{pod}}$	100.0000”	100.0000”	0.0000”
	$\mathbf{Z_{pod}}$	49.1790”	49.1790”	0.0000”
Attach Point 3	$\mathbf{X_{pod}}$	253.5000”	253.5104”	-0.0104”
	$\mathbf{Y_{pod}}$	100.0000”	100.0104”	-0.0104”
	$\mathbf{Z_{pod}}$	39.7680”	39.7784”	-0.0104”

Table 3-5 - Uncertainty due to the tolerances associated with the attach point 3 location on the orbiter.

APS Pod Fitting Locations

There is also uncertainty about the locations of the fittings on the APS pod. As with the orbiter attach point locations, the tolerance associated with the APS pod fitting locations is 0.010”. Therefore, an uncertainty of 0.0104” in all directions is associated with each pod fitting location. The APS pod misalignment caused by this uncertainty is given in Tables 3-6, 3-7 and 3-8.

Attach Point	Coordinate Axis	Nominal Solution	Attach Point 1 Fitting Misalignment of 0.0104” in all three directions	Resulting Attach Point Misalignment
Attach Point 1	$\mathbf{X_{pod}}$	106.5000”	106.5104”	-0.0104”
	$\mathbf{Y_{pod}}$	100.0000”	100.0104”	-0.0104”
	$\mathbf{Z_{pod}}$	152.3460”	152.3564”	-0.0104”
Attach Point 2	$\mathbf{X_{pod}}$	106.5000”	106.5000”	0.0000”
	$\mathbf{Y_{pod}}$	100.0000”	100.0000”	0.0000”
	$\mathbf{Z_{pod}}$	49.1790”	49.1790”	0.0000”
Attach Point 3	$\mathbf{X_{pod}}$	253.5000”	253.5000”	0.0000”

	$\mathbf{Y_{pod}}$	100.0000”	100.0000”	0.0000”
	$\mathbf{Z_{pod}}$	39.7680”	39.7680”	0.0000”

Table 3-6 - Uncertainty due to tolerances associated with the attach point 1 fitting location on the APS pod.

Attach Point	Coordinate Axis	Nominal Solution	Attach Point 2 Fitting Misalignment of 0.0104” in all three directions	Resulting Attach Point Misalignment
Attach Point 1	$\mathbf{X_{pod}}$	106.5000”	106.5000”	0.0000”
	$\mathbf{Y_{pod}}$	100.0000”	100.0000”	0.0000”
	$\mathbf{Z_{pod}}$	152.3460”	152.3460”	0.0000”
Attach Point 2	$\mathbf{X_{pod}}$	106.5000”	106.5104”	-0.0104”
	$\mathbf{Y_{pod}}$	100.0000”	100.0104”	-0.0104”
	$\mathbf{Z_{pod}}$	49.1790”	49.1894”	-0.0104”
Attach Point 3	$\mathbf{X_{pod}}$	253.5000”	253.5000”	0.0000”
	$\mathbf{Y_{pod}}$	100.0000”	100.0000”	0.0000”
	$\mathbf{Z_{pod}}$	39.7680”	39.7680”	0.0000”

Table 3-7 - Uncertainty due to tolerances associated with the attach point 2 fitting location on the APS pod.

Attach Point	Coordinate Axis	Nominal Solution	Attach Point 3 Fitting Misalignment of 0.0104” in all three directions	Resulting Attach Point Misalignment
Attach Point 1	$\mathbf{X_{pod}}$	106.5000”	106.5000”	0.0000”
	$\mathbf{Y_{pod}}$	100.0000”	100.0000”	0.0000”
	$\mathbf{Z_{pod}}$	152.3460”	152.3460”	0.0000”
Attach Point 2	$\mathbf{X_{pod}}$	106.5000”	106.5000”	0.0000”
	$\mathbf{Y_{pod}}$	100.0000”	100.0000”	0.0000”
	$\mathbf{Z_{pod}}$	49.1790”	49.1790”	0.0000”
Attach Point 3	$\mathbf{X_{pod}}$	253.5000”	253.5104”	-0.0104”
	$\mathbf{Y_{pod}}$	100.0000”	100.0104”	-0.0104”
	$\mathbf{Z_{pod}}$	39.7680”	39.7784”	-0.0104”

Table 3-8 - Uncertainty due to tolerances associated with the attach point 3 fitting location on the APS pod.

Lifting Fixture Attach Point 3 Location

The position of the APS pod relative to the lifting fixture is largely determined by the location of the lifting fixture’s attachment to the APS pod attach point 3 fitting.

Drawing tolerances affect the position of the lifting fixture's attachment location relative to the adjustment mechanism end effectors. According to drawing tolerances, the lifting fixture attach point 3 location can be up to (0.0349", 0.0698", 0.0349") from the intended position in (X_{pod}, Y_{pod}, Z_{pod}). It may be surprising to note that this tolerance single-handedly prevents the attach point 3 accuracy requirement from being met. However, it is probable that engineers didn't expect to apply robot kinematics to the lifting fixture when it was designed in 1977. The pod misalignment resulting from this uncertainty can be simply calculated. Results are presented in Table 3-9.

Attach Point	Coordinate Axis	Nominal Solution	Lifting Fixture Attach Point 3 Misalignment Due to Tolerances	Resulting Attach Point Misalignment
Attach Point 1	**X_{pod}**	106.5000"	106.5349"	-0.0349"
	Y_{pod}	100.0000"	100.0698"	-0.0698"
	Z_{pod}	152.3460"	152.3809"	-0.0349"
Attach Point 2	**X_{pod}**	106.5000"	106.5349"	-0.0349"
	Y_{pod}	100.0000"	100.0698"	-0.0698"
	Z_{pod}	49.1790"	49.2139"	-0.0349"
Attach Point 3	**X_{pod}**	253.5000"	253.5349"	-0.0349"
	Y_{pod}	100.0000"	100.0698"	-0.0698"
	Z_{pod}	39.7680"	39.8029"	-0.0349"

Table 3-9 - Uncertainty due to tolerances affecting the lifting fixture attach point 3 location.

Lifting Fixture Adjustment at Attach Point 3

There also exists the capability to adjust the position of the APS pod at the attach point 3 location. The magnitude of this adjustment capability is 0.418" in the $\pm X_{pod}$ directions. Since this adjustment potentially shifts the entire APS pod, all three attach points are affected by this source of uncertainty as shown in Table 3-10 below.

Attach Point	Coordinate Axis	Nominal Solution	Maximum Adjustment of 0.4184” in the $+X_{pod}$ Direction at Attach Point 3	Resulting Attach Point Misalignment
Attach Point 1	X_{pod}	106.5000”	106.9184”	-0.4184”
	Y_{pod}	100.0000”	100.0000”	0.0000”
	Z_{pod}	152.3460”	152.3460”	0.0000”
Attach Point 2	X_{pod}	106.5000”	106.9184”	-0.4184”
	Y_{pod}	100.0000”	100.0000”	0.0000”
	Z_{pod}	49.1790”	49.1790”	0.0000”
Attach Point 3	X_{pod}	253.5000”	253.9184”	-0.4184”
	Y_{pod}	100.0000”	100.0000”	0.0000”
	Z_{pod}	39.7680”	39.7680”	0.0000”

Table 3-10 – Uncertainty due to adjustment capability of lifting fixture-APS pod attachment at the attach point 3 location.

Uncertainty of Input Values

“Garbage in, garbage out.”

-Unknown

Location of Rotator Bar Base

At first glance, it might appear that the base of the rotator bar can be considered “ground” at a known position relative to the spherical joint sockets and orbiter attach points. Unfortunately, this is not the case. One factor is the dimensional variance between each of the three OPFs. The rotator bar base is mounted to a beam in each OPF and the location of that beam might not be identical in each OPF. A much more significant factor is that the position of the orbiter relative to the OPF is not always the same. After each mission, the orbiter is towed into the OPF and jacked off the floor. Per specification, the orbiter must be towed to ±1" forward/aft, ±1.5" port/starboard, and ±0.25" up/down of a specified nominal position. Therefore, the position of the rotator bar base can be significantly different from nominal.

As a result, the position of the rotator bar base relative to the spherical joint sockets must be measured prior to each APS pod installation. Preliminary indications are that this position can be measured to a total accuracy of 0.010" or better. The uncertainty can be determined by positioning the rotator bar base 0.0104" from the nominal position and using nominal joint offsets. The effect of this measurement error is greatest if it occurs along the prismatic joint axis. Table 3-11 below shows the effect of this error on attach point alignment.

Attach Point	Coordinate Axis	Nominal Solution	0.0104" Rotator Base Misalignment	Resulting Attach Point Misalignment
Attach Point 1	$\mathbf{X_{pod}}$	106.5000"	106.4989"	0.0011"
	$\mathbf{Y_{pod}}$	100.0000"	99.9836"	0.0164"
	$\mathbf{Z_{pod}}$	152.3460"	152.3563"	-0.0103"
Attach Point 2	$\mathbf{X_{pod}}$	106.5000"	106.5001"	-0.0001"
	$\mathbf{Y_{pod}}$	100.0000"	99.9974"	0.0026"
	$\mathbf{Z_{pod}}$	49.1790"	49.1893"	-0.0103"
Attach Point 3	$\mathbf{X_{pod}}$	253.5000"	253.5002"	-0.0002"
	$\mathbf{Y_{pod}}$	100.0000"	99.9983"	0.0017"
	$\mathbf{Z_{pod}}$	39.7680"	39.7800"	-0.0120"

Table 3-11 - Uncertainty due to misalignment of rotator bar base.

Calculation-Related Uncertainties

Computer Program Uncertainty

Ideally, the computer program calculates the exact joint offsets required to position the lifting fixture as desired. However, roundoff errors can propagate and potentially become a significant error source.

In order to determine error associated with the program, the lifting fixture CAD model was positioned in a known location. Using Pro/E's mechanism application, connections between components were defined as joints rather than rigid connections. This automatically positioned the adjustment mechanisms and rotator bar joints as needed

to properly connect to the lifting fixture and mechanism base. The position of specific points in the model was then input into the program. The program calculated the joint offsets required to align the lifting fixture. These offsets were compared to the joint offsets measured in the CAD model.

Inaccuracies were initially experienced due to errors in the CAD model. Additionally, using only three decimal places for input values caused significant errors. After these problems had been remedied, numerical methods were not required to further refine the calculations. Results can be viewed in Table 3-12.

Attach Point	Coordinate Axis	Joint Offsets from the CAD Model are Used	Joint Offsets from the Program are Input into the Model	Resulting Attach Point Misalignment
Attach Point 1	$\mathbf{X_{pod}}$	106.5000”	106.5000”	0.0000”
	$\mathbf{Y_{pod}}$	100.0000”	100.0000”	0.0000”
	$\mathbf{Z_{pod}}$	152.3460”	152.3460”	0.0000”
Attach Point 2	$\mathbf{X_{pod}}$	106.5000”	106.5000”	0.0000”
	$\mathbf{Y_{pod}}$	100.0000”	100.0000”	0.0000”
	$\mathbf{Z_{pod}}$	49.1790”	49.1790”	0.0000”
Attach Point 3	$\mathbf{X_{pod}}$	253.5000”	253.5000”	0.0000”
	$\mathbf{Y_{pod}}$	100.0000”	100.0000”	0.0000”
	$\mathbf{Z_{pod}}$	39.7680”	39.7680”	0.0000”

Table 3-12 - Uncertainty due to inaccurate calculations by the program.

Hardware Positioning Uncertainty

Although joint offsets can be accurately calculated to several decimal places, the ability of the pod installation team to adjust the rotator bar and adjustment mechanisms is limited. These limitations are largely due to measurement device uncertainty, mounting inaccuracies, and the tolerances of the components being measured.

Uphill/Downhill Joint Offset Measurement

The joint offset S_4 has been previously defined as the distance along the $\overrightarrow{S_4}$ vector between the $\overrightarrow{a_{34}}$ and $\overrightarrow{a_{45}}$ vectors. The pod installation team can adjust this joint offset to match the value calculated by the alignment program.

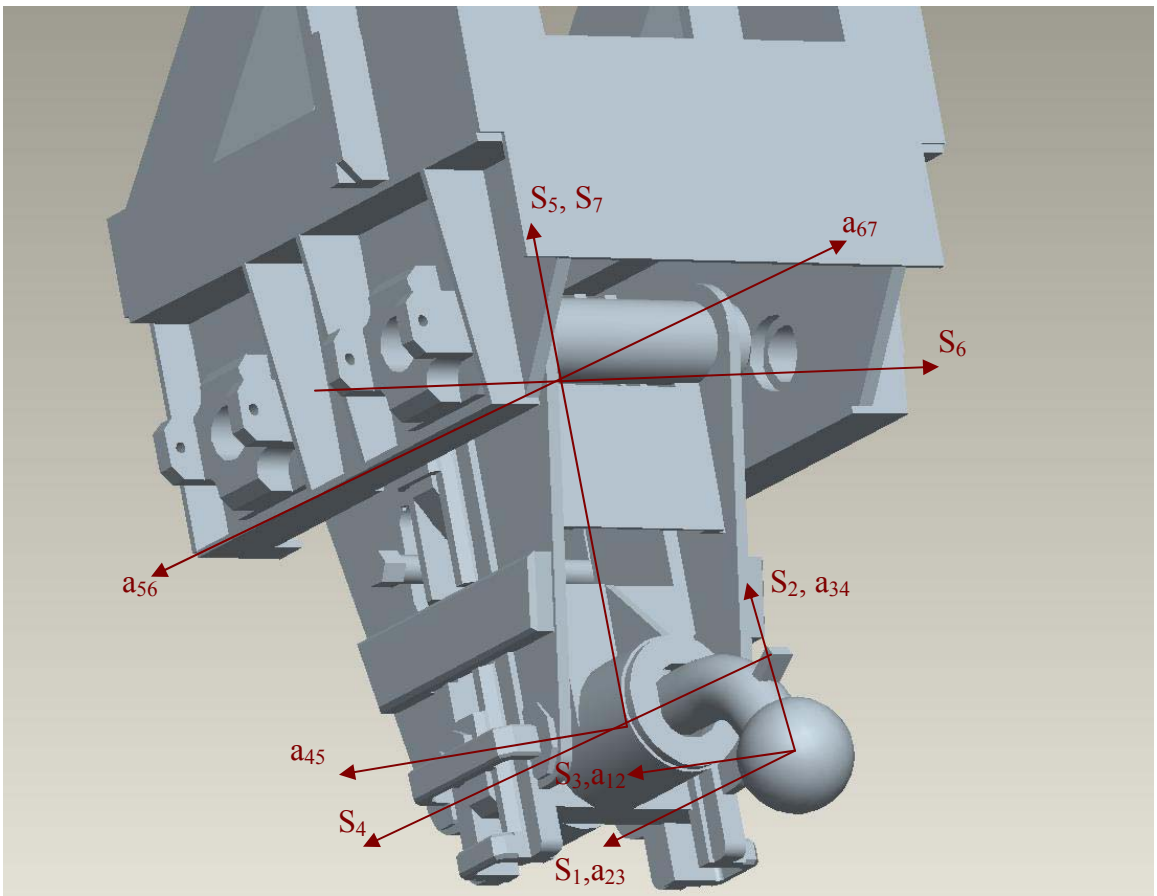

Figure 3-1 - Adjustment mechanism joint axis vectors and link vectors.

The desired joint offset reading on the measurement device can be achieved. However, the accuracy of this measurement is affected by factors such as measurement device uncertainty, mounting inaccuracies, and hardware tolerances. A preliminary assessment of these factors suggests that an accuracy of ±0.010" can be achieved. This uncertainty analysis will determine the alignment error resulting from a misalignment of

0.0104” uphill for the forward and aft adjustment mechanism. The results of this analysis are stated below in Tables 3-13 and 3-14.

Attach Point	Coordinate Axis	Nominal Solution	Misalignment of the Fwd S_4 0.0104” Uphill	Resulting Attach Point Misalignment
Attach Point 1	$\mathbf{X_{pod}}$	106.5000”	106.5071”	-0.0071”
	$\mathbf{Y_{pod}}$	100.0000”	100.0080”	-0.0080”
	$\mathbf{Z_{pod}}$	152.3460”	152.3686”	-0.0226”
Attach Point 2	$\mathbf{X_{pod}}$	106.5000”	106.5011”	-0.0011”
	$\mathbf{Y_{pod}}$	100.0000”	100.0005”	-0.0005”
	$\mathbf{Z_{pod}}$	49.1790”	49.2015”	-0.0225”
Attach Point 3	$\mathbf{X_{pod}}$	253.5000”	253.5005”	-0.0005”
	$\mathbf{Y_{pod}}$	100.0000”	99.9996”	0.0004”
	$\mathbf{Z_{pod}}$	39.7680”	39.7819”	-0.0139”

Table 3-13 - Uncertainty due to misalignment of the forward adjustment mechanism by 0.0104” uphill.

Attach Point	Coordinate Axis	Nominal Solution	Misalignment of the Aft S_4 0.0104” Uphill	Resulting Attach Point Misalignment
Attach Point 1	$\mathbf{X_{pod}}$	106.5000”	106.4929”	0.0071”
	$\mathbf{Y_{pod}}$	100.0000”	100.0058”	-0.0058”
	$\mathbf{Z_{pod}}$	152.3460”	152.3550”	-0.0090”
Attach Point 2	$\mathbf{X_{pod}}$	106.5000”	106.4992”	0.0008”
	$\mathbf{Y_{pod}}$	100.0000”	100.0003”	-0.0003”
	$\mathbf{Z_{pod}}$	49.1790”	49.1880”	-0.0090”
Attach Point 3	$\mathbf{X_{pod}}$	253.5000”	253.4999”	0.0001”
	$\mathbf{Y_{pod}}$	100.0000”	99.9994”	0.0006”
	$\mathbf{Z_{pod}}$	39.7680”	39.7860”	-0.0180”

Table 3-14 - Uncertainty due to misalignment of the aft adjustment mechanism by 0.0104" uphill.

Off-the-Deck/On-the-Deck Joint Offset Measurement

The accuracy of the S_5 joint offset measurement is also affected by measurement device uncertainty, mounting inaccuracies, and hardware tolerances. The total measurement uncertainty is approximated as $\pm 0.010"$. An analysis has been performed to ascertain attach point misalignment due to a 0.0104” misalignment in the off-the-deck

direction for each adjustment mechanism. The results of this analysis can be found in Tables 3-15 and 3-16.

Attach Point	Coordinate Axis	Nominal Solution	Misalignment of the Fwd S_5 0.0104" Off-the-Deck	Resulting Attach Point Misalignment
Attach Point 1	X_{pod}	106.5000"	106.5002"	-0.0002"
	Y_{pod}	100.0000"	100.0103"	-0.0103"
	Z_{pod}	152.3460"	152.3566"	-0.0106"
Attach Point 2	X_{pod}	106.5000"	106.5006"	-0.0006"
	Y_{pod}	100.0000"	100.0113"	-0.0113"
	Z_{pod}	49.1790"	49.1895"	-0.0105"
Attach Point 3	X_{pod}	253.5000"	253.5007"	-0.0007"
	Y_{pod}	100.0000"	100.0023"	-0.0023"
	Z_{pod}	39.7680"	39.7792"	-0.0112"

Table 3-15 - Uncertainty due to misalignment of the fwd adjustment mechanism by 0.0104" off-the-deck.

Attach Point	Coordinate Axis	Nominal Solution	Misalignment of the Aft S_5 0.0104" Off-the-Deck	Resulting Attach Point Misalignment
Attach Point 1	X_{pod}	106.5000"	106.4993"	0.0007"
	Y_{pod}	100.0000"	99.9961"	0.0039"
	Z_{pod}	152.3460"	152.3570"	-0.0110"
Attach Point 2	X_{pod}	106.5000"	106.4996"	0.0004"
	Y_{pod}	100.0000"	99.9978"	0.0022"
	Z_{pod}	49.1790"	49.1900"	-0.0110"
Attach Point 3	X_{pod}	253.5000"	253.4996"	0.0004"
	Y_{pod}	100.0000"	100.0063"	-0.0063"
	Z_{pod}	39.7680"	39.7795"	-0.0115"

Table 3-16 - Uncertainty due to misalignment of the aft adjustment mechanism by 0.0104" off-the-deck.

Forward/Aft Joint Offset Measurement

As with the measurement uncertainties for joint offsets S_4 and S_5, it is assumed that measurements of joint offset S_6 are accurate to within 0.010". The effect of a 0.0104" misalignment in the forward direction was studied. In order for this misalignment to occur, the entire lifting fixture must be 0.0104" forward which means

both the forward and aft S_6 are misaligned by the same value. The resulting misalignment of attach points is listed in Table 3-17.

Attach Point	Coordinate Axis	Nominal Solution	Misalignment of the Fwd S_6 and Aft S_6 by 0.0104" in the Forward Direction	Resulting Attach Point Misalignment
Attach Point 1	$\mathbf{X_{pod}}$	106.5000"	106.4997"	0.0003"
	$\mathbf{Y_{pod}}$	100.0000"	99.9992"	0.0008"
	$\mathbf{Z_{pod}}$	152.3460"	152.3565"	-0.0105"
Attach Point 2	$\mathbf{X_{pod}}$	106.5000"	106.5002"	-0.0002"
	$\mathbf{Y_{pod}}$	100.0000"	99.9995"	0.0005"
	$\mathbf{Z_{pod}}$	49.1790"	49.1895"	-0.0105"
Attach Point 3	$\mathbf{X_{pod}}$	253.5000"	253.5002"	-0.0002"
	$\mathbf{Y_{pod}}$	100.0000"	99.9992"	0.0008"
	$\mathbf{Z_{pod}}$	39.7680"	39.7792"	-0.0112"

Table 3-17 - Uncertainty due to misalignment of the fwd and aft adjustment mechanisms by 0.0104" in the forward direction.

Rotator Bar Joint Offset Measurement

The rotator bar S_3 prismatic joint offset is affected by the same uncertainty sources as the adjustment mechanism joint offsets. Measurement uncertainty is also approximately ±0.010". The misalignment of a rotator bar that is extended 0.0104" more than the measurement indicates is depicted in Table 3-18.

Attach Point	Coordinate Axis	Nominal Solution	Misalignment of the Rotator Bar S_3 0.0104" Extend	Resulting Attach Point Misalignment
Attach Point 1	$\mathbf{X_{pod}}$	106.5000"	106.4989"	0.0011"
	$\mathbf{Y_{pod}}$	100.0000"	99.9836"	0.0164"
	$\mathbf{Z_{pod}}$	152.3460"	152.3563"	-0.0103"
Attach Point 2	$\mathbf{X_{pod}}$	106.5000"	106.5001"	-0.0001"
	$\mathbf{Y_{pod}}$	100.0000"	99.9974"	0.0026"
	$\mathbf{Z_{pod}}$	49.1790"	49.1893"	-0.0103"
Attach Point 3	$\mathbf{X_{pod}}$	253.5000"	253.5002"	-0.0002"
	$\mathbf{Y_{pod}}$	100.0000"	99.9983"	0.0017"
	$\mathbf{Z_{pod}}$	39.7680"	39.7800"	-0.0120"

Table 3-18 - Uncertainty due to misalignment of the rotator bar by 0.0104" in the extend direction.

Compliance in Joints

It is stated in [2] that "80% of the flexibility of industrial robots comes from the joint". Quantifying this compliance is a difficult task. It will be estimated by considering each joint on an individual basis. Joints exist where two components are attached. The dimensional difference between those two components was first identified. Loading was then considered while determining the relative position of the components under the assumption they are in contact. One component is translated and, in some cases also rotated, to the determined position. The resulting APS pod misalignment is calculated from these translations and rotations. The total uncertainty related to compliance is documented in Table 3-19.

Attach Point	Coordinate Axis	Nominal Solution	Attach Point Misalignment
Attach Point 1	$\mathbf{X_{pod}}$	106.5000"	0.0022"
	$\mathbf{Y_{pod}}$	100.0000"	0.3914"
	$\mathbf{Z_{pod}}$	152.3460"	0.1172"
Attach Point 2	$\mathbf{X_{pod}}$	106.5000"	0.0002"
	$\mathbf{Y_{pod}}$	100.0000"	0.0886"
	$\mathbf{Z_{pod}}$	49.1790"	0.0628"
Attach Point 3	$\mathbf{X_{pod}}$	253.5000"	0.0004"
	$\mathbf{Y_{pod}}$	100.0000"	0.0955"
	$\mathbf{Z_{pod}}$	39.7680"	0.0620"

Table 3-19 - Uncertainty due to joint compliance.

Total Uncertainty Calculation

There are different methods for calculating total system uncertainty for a specified set of individual uncertainties. Individual uncertainties at each attach point are summarized in Tables 3-20, 3-21, and 3-22. This information will be used to calculate total uncertainty using the 100% covariance method and the least squared method. The

total uncertainty will subsequently be compared to the accuracy requirements for APS pod alignment.

Uncertainty Description	Attach Point 1 (inches)		
	X_{pod}	Y_{pod}	Z_{pod}
Fwd spherical joint socket location	0.0003	0.0008	0.0105
Aft spherical joint socket location	0.0003	0.0008	0.0105
Orbiter attach point 1 location	0.0104	0.0104	0.0104
Orbiter attach point 2 location	0.0000	0.0000	0.0000
Orbiter attach point 3 location	0.0000	0.0000	0.0000
APS pod attach point 1 location	0.0104	0.0104	0.0104
APS pod attach point 2 location	0.0000	0.0000	0.0000
APS pod attach point 3 location	0.0000	0.0000	0.0000
Lifting fixture nominal attach point 3 location	0.0349	0.0698	0.0349
Adjustment capability of attach point 3	0.4184	0.0000	0.0000
Measurement of rotator bar base location	0.0011	0.0164	0.0103
Calculations by computer program	0.0000	0.0000	0.0000
Iterative process acceptance criteria	0.0005	0.0005	0.0004
Measurement of fwd adjustment mechanism uphill/downhill position	0.0071	0.0080	0.0226
Measurement of aft adjustment mechanism uphill/downhill position	0.0071	0.0058	0.0090
Measurement of fwd adjustment mechanism off-the-deck/on-the-deck position	0.0002	0.0103	0.0106
Measurement of aft adjustment mechanism off-the-deck/on-the-deck position	0.0007	0.0039	0.0110
Measurement of adjustment mechanism forward/aft position	0.0003	0.0008	0.0105
Measurement of rotator bar joint offset	0.0011	0.0164	0.0103
Compliance in joints	0.0022	0.3914	0.1172

Table 3-20 - Summary of uncertainty sources at attach point 1.

Uncertainty Description	Attach Point 2 (inches)		
	X_{pod}	Y_{pod}	Z_{pod}
Fwd spherical joint socket location	0.0002	0.0005	0.0105
Aft spherical joint socket location	0.0002	0.0005	0.0105
Orbiter attach point 1 location	0.0000	0.0000	0.0000
Orbiter attach point 2 location	0.0104	0.0104	0.0104
Orbiter attach point 3 location	0.0000	0.0000	0.0000
APS pod attach point 1 location	0.0000	0.0000	0.0000
APS pod attach point 2 location	0.0104	0.0104	0.0104
APS pod attach point 3 location	0.0000	0.0000	0.0000

Lifting fixture nominal attach point 3 location	0.0349	0.0698	0.0349
Adjustment capability of attach point 3	0.4184	0.0000	0.0000
Measurement of rotator bar base location	0.0001	0.0026	0.0103
Computer program roundoff error	0.0000	0.0000	0.0000
Iterative process acceptance criteria	0.0001	0.0005	0.0004
Measurement of fwd adjustment mechanism uphill/downhill position	0.0011	0.0005	0.0225
Measurement of aft adjustment mechanism uphill/downhill position	0.0008	0.0003	0.0090
Measurement of fwd adjustment mechanism off-the-deck/on-the-deck position	0.0006	0.0113	0.0105
Measurement of aft adjustment mechanism off-the-deck/on-the-deck position	0.0004	0.0022	0.0110
Measurement of adjustment mechanism forward/aft position	0.0002	0.0005	0.0105
Measurement of rotator bar joint offset	0.0001	0.0026	0.0103
Compliance in joints	0.0002	0.0886	0.0628

Table 3-21 - Summary of uncertainty sources at attach point 2.

Uncertainty Description	**Attach Point 3 (inches)**		
	$\mathbf{X_{pod}}$	$\mathbf{Y_{pod}}$	$\mathbf{Z_{pod}}$
Fwd spherical joint socket location	0.0002	0.0008	0.0112
Aft spherical joint socket location	0.0002	0.0008	0.0112
Orbiter attach point 1 location	0.0000	0.0000	0.0000
Orbiter attach point 2 location	0.0000	0.0000	0.0000
Orbiter attach point 3 location	0.0104	0.0104	0.0104
APS pod attach point 1 location	0.0000	0.0000	0.0000
APS pod attach point 2 location	0.0000	0.0000	0.0000
APS pod attach point 3 location	0.0104	0.0104	0.0104
Lifting fixture nominal attach point 3 location	0.0349	0.0698	0.0349
Adjustment capability of attach point 3	0.4184	0.0000	0.0000
Measurement of rotator bar base location	0.0002	0.0017	0.0120
Computer program roundoff error	0.0000	0.0000	0.0000
Iterative process acceptance criteria	0.0001	0.0005	0.0001
Measurement of fwd adjustment mechanism uphill/downhill position	0.0005	0.0004	0.0139
Measurement of aft adjustment mechanism uphill/downhill position	0.0001	0.0006	0.0180
Measurement of fwd adjustment mechanism off-the-deck/on-the-deck position	0.0007	0.0023	0.0112
Measurement of aft adjustment mechanism off-the-deck/on-the-deck position	0.0004	0.0063	0.0115
Measurement of adjustment mechanism forward/aft position	0.0002	0.0008	0.0112
Measurement of rotator bar joint offset	0.0002	0.0017	0.0120

Compliance in joints	0.0004	0.0955	0.0620

Table 3-22 - Summary of uncertainty sources at attach point 3.

100% Covariance Method

The 100% covariance method assumes that each individual uncertainty is at a maximum at the same time. Assuming that all significant sources of uncertainty have been found and reasonably approximated, the 100% covariance method provides the "worst case scenario".

The total uncertainty is calculated by summing all individual uncertainties. The X_{pod} and Z_{pod} accuracy requirements at attach points 1 and 3 are not specified individually. Since it is desired to compare total uncertainty to accuracy requirements, the X_{pod} and Z_{pod} total uncertainty has been combined for attach points 1 and 3. Table 3-23 allows the uncertainty calculated using the 100% covariance method to be compared to the accuracy requirement.

	Attach Point 1 (inches)		**Attach Point 2 (inches)**			**Attach Point 3 (inches)**	
Description	**X_{pod}/Z_{pod}**	**Y_{pod}**	**X_{pod}**	**Y_{pod}**	**Z_{pod}**	**X_{pod}/Z_{pod}**	**Y_{pod}**
Total Uncertainty	0.5680	0.5457	0.4781	0.2007	0.2240	0.5298	0.2020
Accuracy Requirement	0.2190	0.0010	2.0000	0.0010	0.0093	0.0033	0.0010
Remaining Margin	**-0.3490**	**-0.5447**	**1.5219**	**-0.1997**	**-0.2147**	**-0.5265**	**-0.2010**

Table 3-23 - Total uncertainty as calculated by the 100% covariance method.

Root Sum Squared Method

The root sum squared method provides the lower bound for total uncertainty projections. The root sum squared uncertainty is calculated by

$$U_{Total} = \sqrt{\sum_{i=1}^{n} U_i^2} \qquad (3.1)$$

where U_{Total} is the total uncertainty and the individual uncertainties are given by U_i through U_n.

The X_{pod} and Z_{pod} uncertainties at attach points 1 and 3 have been combined for comparison to accuracy requirements. This comparison is presented in Table 3-24.

	Attach Point 1 (inches)		**Attach Point 2 (inches)**			**Attach Point 3 (inches)**	
Description	**X_{pod}/Z_{pod}**	**Y_{pod}**	**X_{pod}**	**Y_{pod}**	**Z_{pod}**	**X_{pod}/Z_{pod}**	**Y_{pod}**
Total Uncertainty	0.4395	0.3988	0.4201	0.1144	0.0821	0.4280	0.1194
Accuracy Requirement	0.2190	0.0010	2.0000	0.0010	0.0093	0.0033	0.0010
Remaining Margin	**-0.2205**	**-0.3978**	**1.5799**	**-0.1134**	**-0.0728**	**-0.4247**	**-0.1184**

Table 3-24 - Total uncertainty as calculated using the root sum squared method.

CHAPTER 4
EVALUATION OF PROPOSED ALIGNMENT METHOD

Both uncertainty calculation methods employed in Chapter 3 indicate that the proposed solution method is not as accurate as desired. If used, it would not be able to align the APS pod with the orbiter deck accurately enough to eliminate the need for additional manipulations. The additional manipulations required for alignment can not be calculated before the operation because the direction and magnitude of the misalignment can not be predicted. Additional manipulations are highly undesirable because the motion resulting from mechanism adjustments is not intuitive. As a result, the uncertainty analysis will be further examined and recommendations will be made to reduce total uncertainty.

Discussion of Results

Uncertainty due to tolerances can be significantly reduced by measuring "as-built" dimensions. The uncertainty associated with those measurements is significantly less than the uncertainty due to tolerances, in some cases by more than one order of magnitude. Measurements of specific points on the lifting fixture, APS pod, and orbiter can be taken prior to the APS pod installation.

Uncertainty can be further reduced by more accurately measuring rotator bar joint offset S_5 and adjustment mechanism joint offsets S_4, S_5, and S_6. Improvements to reduce uncertainty might require significant modifications to rotator bar and adjustment mechanism hardware. However, these modifications are highly desirable because the

uncertainty associated with *each* joint offset measurement exceeds the total allowable uncertainty at attach point 3 by one order of magnitude.

The estimated uncertainty due to compliance in rotator bar and adjustment mechanism joints is one of the most significant error sources studied. Although joint compliance can not be reduced without significant modifications to hardware, its effect can be minimized. There are only two lifting fixtures, one for right APS pods and one for left APS pods, and those lifting fixtures are in approximately the same position and orientation during each APS pod installation. The geometry of the lifting fixture configuration indicates that each joint is under load during this operation and those loads determine the direction affected by compliance. As a result, joint compliance has only a minimal effect on precision. In order to obtain accurate results, a correction factor can be used to compensate for joint compliance error.

A correction factor might also be used to compensate for uncertainties related to lifting fixture, APS pod, and orbiter geometry. For a given lifting fixture, APS pod, and orbiter it might be discovered that the calculated solution results in a misalignment that is consistent in magnitude and direction. This precise solution could be made more accurate by implementing a correction factor. Since there are only two lifting fixtures, three orbiters, and a small number of APS pods, a database could be created relatively quickly to facilitate the calculation of a correction factor for each scenario.

Recommendations

The lifting fixture, adjustment mechanisms, and rotator bar are not currently outfitted with a means of measuring joint offsets. Therefore, it is suggested that measurement devices for each joint offset be installed. Laser rangefinders should be considered because they provide high accuracy and can be installed without modifying

load-bearing components. The proposed solution method will allow the shuttle team to align the APS pod by manipulating joints to pre-calculated positions. Without measurement devices, the shuttle team will not know when the pre-calculated positions have been reached. Based on an uncertainty analysis, an accuracy of ±0.010" is insufficient for measurement devices. Overall system accuracy would be greatly improved if measurement device accuracy approached ±0.001". Crude measurement techniques such a rulers or tape measures would provide highly inaccurate results.

The lifting fixture design includes adjustment capability at all attach points to accommodate APS pod dimensional variation. This adjustment capability is large enough that it must be accounted for when considering the location of the APS pod relative to reference points on the lifting fixture. The simplest and most accurate method of determining the position of the APS pod relative to the lifting fixture is to make high-accuracy measurements before each APS pod is installed. APS pod attach points 1, 2, and 3 must be measured as well as the rotator bar and adjustment mechanism end effector locations. Since the orientation of the adjustment mechanism end effectors must be known, a second point along each adjustment mechanism $\overrightarrow{S_6}$ and $\overrightarrow{a_{67}}$ vectors must also be measured.

Total uncertainty can be further reduced by making additional high-accuracy measurements of the rotator bar base and spherical joint socket locations. Orbiter attach point positions can be similarly determined. These measurements yield only marginal accuracy improvements but are desirable nonetheless. In general, high-accuracy measurements can be used to compensate for insufficiently loose tolerances.

As previously mentioned, a hydraulic jack is used to ensure the aft adjustment mechanism "follows" the forward adjustment mechanism during forward/aft motion of the lifting fixture. The hydraulic jack is not a precise method for positioning the aft adjustment mechanism. The adjustment mechanisms could be more accurately positioned in the forward/aft direction before they are installed in the sockets. Since the adjustment mechanisms will not be supporting the weight of the lifting fixture or APS pod at that point, they can be adjusted to the pre-calculated solution position without experiencing binding. If the S_6 joint offset calculations are correct, the adjustment mechanisms will not need to be adjusted in the forward/aft direction during operations.

One advantage of the proposed solution method is that joint offset adjustments do not need to be made in any particular sequence. Therefore, it is not imperative that motions be simultaneous with one exception. As the APS pod is lowered to the orbiter deck, the bottom of the APS pod should be approximately parallel to the orbiter deck surface. If one bulb seal compresses before the others make contact, then the resulting frictional force might cause a slight misalignment. To minimize this effect, a reverse kinematic analysis should also be performed to position the APS pod at a waypoint 1/8" above the orbiter deck and aligned in X_{pod} and Z_{pod}. The APS pod can be slowly lowered onto the deck from that waypoint by simultaneously adjusting the rotator bar and adjustment mechanisms.

It would also be beneficial to calculate the joint angle adjustments needed to move the APS pod in small increments along each axis. If the lifting fixture is manipulated to the pre-calculated joint angles and found to be misaligned, the shuttle team will know how to manipulate the lifting fixture to align the APS pod rather than rely on intuition.

A finite element analysis should be performed on the lifting fixture with the APS pod in the installed position. This will allow the rigid body assumption to be validated. If the FEA shows that lifting fixture deflection is significant, then the deflected lifting fixture shape will be used throughout reverse kinematic analysis calculations.

Summary of Recommendations

I. Install measurement devices to measure all variable joint offsets.
II. Make high-accuracy measurements (±0.001") of all critical relative positions.
III. Position the adjustment mechanisms in the forward/aft direction per S_6 joint offset solutions before they begin supporting lifting fixture and APS pod weight.
IV. The APS pod should be positioned at a waypoint 1/8” above the orbiter deck and aligned along the plane of the orbiter deck. The joint offsets needed to position the pod at the waypoint are calculated by reverse kinematic analysis.
V. Joint angle adjustments for small misalignments along each pod coordinate axis should be utilized.
VI. Perform FEA to validate the rigid body assumption.

Conclusions

It should be evident at this point that the design of the lifting fixture, adjustment mechanisms, and rotator bar is not adequate for the precision positioning task it is required to perform. Given the shuttle program’s limited resources, it is highly unlikely that this GSE will be redesigned to improve operations in lieu of upgrades to flight hardware. The reverse kinematic analysis presented in this thesis does not add the desired level of accuracy to the APS pod alignment operation. However, the level of accuracy it does provide is a substantial improvement to the current process.

Implementation of this solution method adds a relatively small amount of manpower and cost to operations compared to the projected benefit. This solution method is a viable aid to APS pod alignment during installation onto the orbiter.

APPENDIX A
TERMS AND ACRONYMS

Table A.1 contains an alphabetical listing of terms and acronyms used throughout this thesis that might not be familiar to this thesis' audience.

Term or Acronym	Definition
Adjustment Mechanisms	Two PPPS manipulators used for OMS pod alignment.
APS	Aft Propulsion System
APS Pod	Orbiter component that houses the Orbital Maneuvering System and the aft Reaction Control System.
Cylinder Joint	A joint that allows rotational and translational motion about the same axis.
FEA	Finite Element Analysis
GSE	Ground Support Equipment
Hydraulic Jack	A force-output device used to overcome the binding condition experienced by the aft adjustment mechanism and cause forward/aft motion along a prismatic joint axis.
Hypergol	A rocket fuel that spontaneously ignites when mixed with an oxidizer. Monomethyl hydrazine is the hypergol used by the OMS.
KSC	Kennedy Space Center
Lifting Fixture	A large structure that attaches to the OMS pod and is manipulated by the adjustment mechanisms and rotator bar.

Move Director	The USA technician that uses information from technicians and engineers to determine the next manipulation.
NASA	National Aeronautics and Space Administration
Nominal Solution	The joint offsets required to align the lifting fixture.
OMS	Orbiter Maneuvering System, propulsion system that provides thrust for orbital insertion, orbit circularization, orbit transfer, rendezvous, and deorbit [12].
OPF	Orbiter Processing Facility
Orbiter Deck	The orbiter surface that mates to the OMS pod.
Plücker Coordinates	Homogeneous coordinates used to describe points, lines, or planes. Plücker coordinates can be used to simplify equations so that calculations can be performed more efficiently.
Prismatic Joint	A joint that allows translational motion only (also known as a slider joint).
Pro/E	Pro/ENGINEER, a CAD software package used for modeling and finite element analysis.
RCS	Reaction Control System, propulsion system used as the primary flight control at altitudes greater than 70,000 feet [12].
Revolute Joint	A joint that allows rotational motion only (also known as a hinge joint).
Rotator Bar	A RRPRRR manipulator used for OMS pod alignment.
Spherical Joint	A joint that allows rotational motion in x, y, and z directions (also known as a ball-and-socket joint).
USA	United Space Alliance, a Boeing and Lockheed Martin joint venture. USA is the prime contractor for space shuttle operations.

Table A.1 – Definitions of terms and acronyms.

APPENDIX B
SHUTTLE COORDINATE SYSTEMS

Several different coordinate systems are commonly used to describe locations on the space shuttle. Two of these coordinate systems are the orbiter coordinate system and the APS pod coordinate system.

The orbiter coordinate system is essentially the orbiter's version of a body-fixed coordinate system. The origin is located forward of the orbiter's nose. The positive X-direction is aft, positive Y- direction is outboard through the starboard wing, and positive Z- direction is out through the vertical tail. The location and orientation of the orbiter coordinate system can be seen in Figure B-1. Orbiter coordinates are used throughout this analysis except when the location of the orbiter deck is specifically needed.

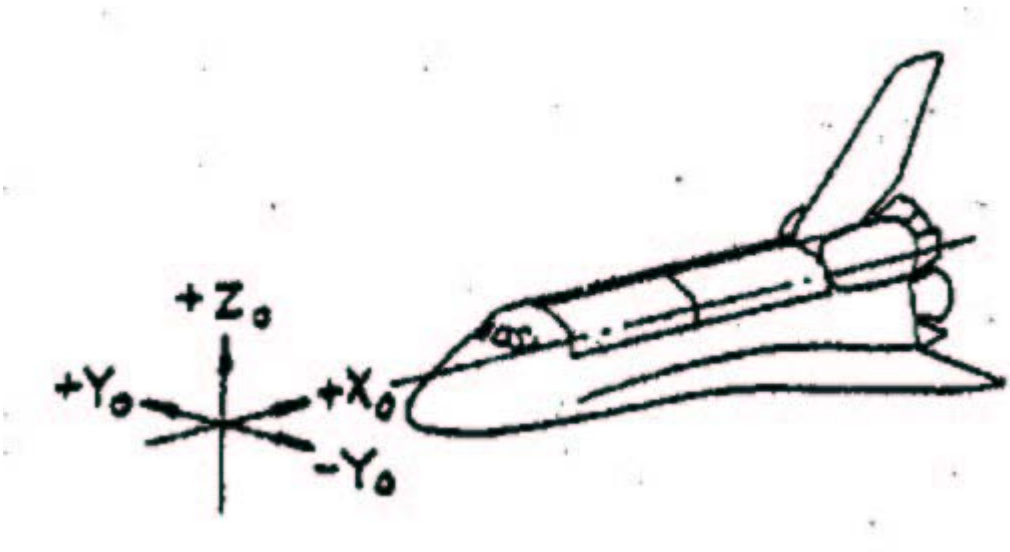

Figure B-1 - Orbiter coordinate system.

The APS pod coordinate systems are local coordinate systems used to describe orbiter locations relative to the orbiter deck planes. In both right APS pod coordinates and left APS pod coordinates, the plane of the appropriate orbiter deck can be described by the equation $Y_{pod} = 100$. The origin is located forward of the APS pod and below the orbiter deck. The positive X- direction is aft and slightly outboard, positive Y- direction is perpendicular to the orbiter deck and includes an outboard component, and positive Z-

direction is angled inboard along the plane of the orbiter deck. The right APS pod coordinate system can be seen in Figure B-2.

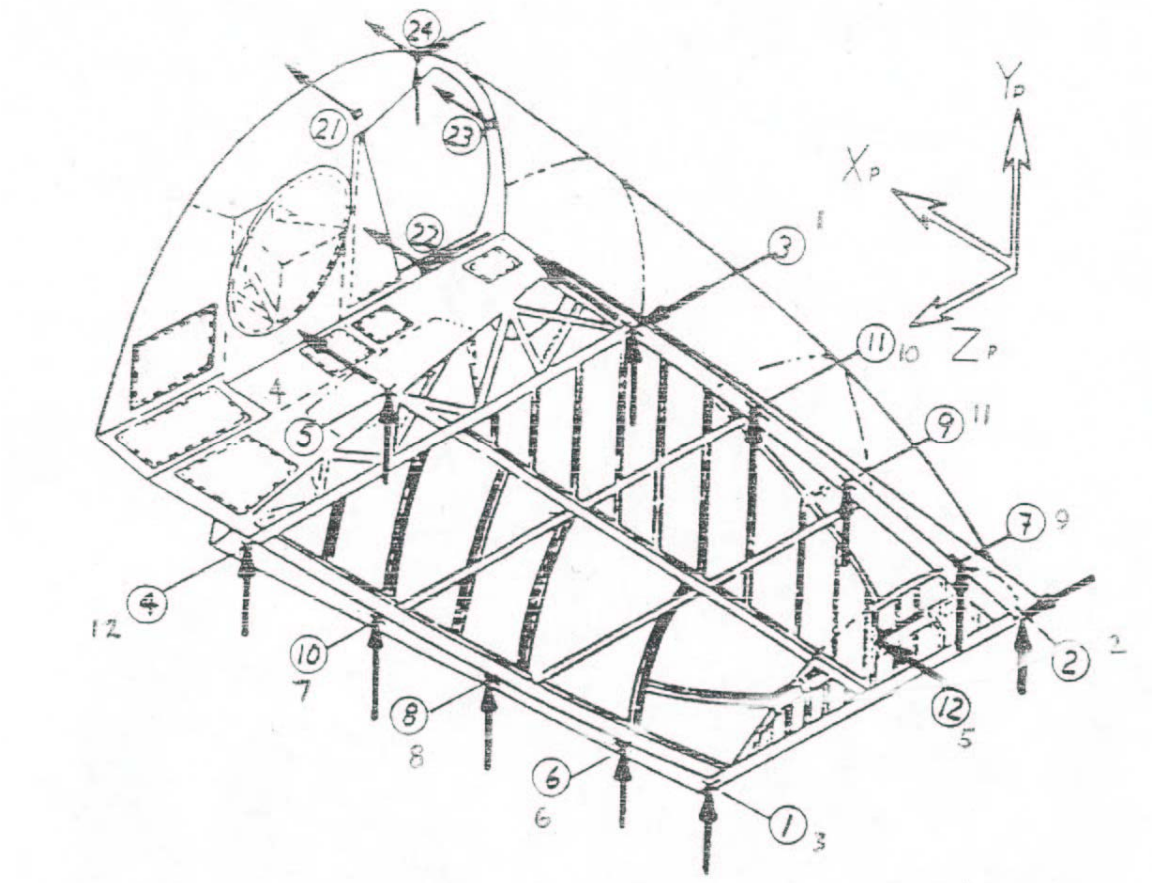

Figure B.2 - Right APS pod coordinate system.

The transformation matrices between orbiter coordinates and right APS pod coordinates are documented as

$$
{}^{Orbiter}_{RightPod}T = \begin{bmatrix} 0.9986104865 & -0.0526981625 & 0 & 1212.4087676 \\ 0.0379078857 & 0.7183402679 & 0.6946583705 & 59.30094352 \\ 0.0366072197 & 0.6936931332 & 0.7193398003 & 311.74989638 \\ 0 & 0 & 0 & 1 \end{bmatrix}
$$

$$
{}^{RightPod}_{Orbiter}T = \begin{bmatrix} 0.9986104865 & 0.0379078857 & 0.0366072197 & -1224.3843795 \\ -0.0526981625 & 0.7183402679 & 0.6936931332 & -194.96530381 \\ 0 & -0.6946583705 & 0.7193398003 & -183.06021143 \\ 0 & 0 & 0 & 1 \end{bmatrix} \quad \text{(B.1)}
$$

Drawings containing the APS pod and its ground support equipment show hardware associated with the left APS pod. The CAD model is based on these drawings and therefore also depicts left APS pod hardware. Unfortunately, transformation matrices for the left APS pod coordinate system are not documented.

The location and orientation of the APS pod coordinate systems are symmetric about the orbiter coordinate XZ plane. Using this fact, transformation matrices for the left APS pod coordinate system can be calculated.

It should be noted that the left APS pod coordinate system does not obey the right hand rule. In the interest of avoiding calculation errors due to the use of a left hand coordinate system, the derived left APS pod coordinate system will be made to obey the right hand rule by inverting its Z- axis.

First, the rotation angle θ about unknown unit vector $\vec{m}$ can be calculated from

$$
\theta = \cos^{-1}\left(\frac{r_{11} + r_{22} + r_{33} - 1}{2}\right) = 44.0984373537^{\circ} \quad \text{(B.2)}
$$

where r_{11}, r_{22}, and r_{33} are the first three diagonal terms in ${}^{Orbiter}_{RightPod}T$. The unit vector $\vec{m}$ can be determined from

$$
\begin{aligned}
m_x &= \pm\sqrt{\frac{r_{11}-\cos\theta}{1-\cos\theta}} = \pm 0.997532008229 \\
m_y &= \frac{r_{12}+r_{21}}{2m_x\left(1-\cos\theta\right)} = \pm 0.026302324052 \\
m_z &= \frac{r_{13}+r_{31}}{2m_x\left(1-\cos\theta\right)} = \pm 0.065100540004
\end{aligned}
\tag{B.3}
$$

The sign of m_x and subsequent signs of m_y and m_z are determined from

$$
\begin{aligned}
m_x &= \frac{r_{32}-r_{23}}{2\sin\theta} = -0.997532008229 \\
m_y &= -0.026302324052 \\
m_z &= -0.065100540004
\end{aligned}
\tag{B.4}
$$

To calculate the left APS pod coordinate system, a rotation of -θ about the mirror of vector $\vec{m}$ will be conducted. The resulting transformation matrix is

$$
{}^{Orbiter}_{LeftPod}T = \begin{bmatrix}
m_x m_x \upsilon + \cos\theta & -m_x m_y \upsilon - m_z \sin\theta & m_x m_z \upsilon - m_y \sin\theta & -1224.380 \\
-m_x m_y \upsilon + m_z \sin\theta & m_y m_y \upsilon + \cos\theta & -m_y m_z \upsilon - m_x \sin\theta & -194.965 \\
m_x m_z \upsilon + m_y \sin\theta & -m_y m_z \upsilon + m_x \sin\theta & m_z m_z \upsilon + \cos\theta & 183.060 \\
0 & 0 & 0 & 1
\end{bmatrix} \tag{B.5}
$$

$$\upsilon \equiv 1-\cos\theta = 0.2818547227$$

After altering the matrix to invert the Z- axis, the result is

$$
{}^{Orbiter}_{LeftPod}T = \begin{bmatrix}
0.9986104865 & -0.0379078857 & 0.0366072197 & -1224.380 \\
-0.0526981625 & -0.7183402679 & 0.6936931333 & -194.965 \\
0 & -0.6946583705 & -0.7193398003 & 183.060 \\
0 & 0 & 0 & 1
\end{bmatrix} \tag{B.6}
$$

The inverse of this matrix is

$$
{}^{Orbiter}_{LeftPod}T = \begin{bmatrix}
0.9986104864 & -0.0526981625 & 0 & 1212.40876751 \\
-0.03790788569 & -0.718340267955 & -0.694658370457 & -59.3009435119 \\
0.036607219672 & 0.693693133334 & -0.71933980034 & 311.749896399 \\
0 & 0 & 0 & 1
\end{bmatrix} \tag{B.7}
$$

In retrospect, the simplest solution would have been to have the program invert all negative orbiter Y- coordinates input into the program. This would have eliminated the need for the left APS pod coordinate derivation because the right APS pod coordinate system could be utilized instead.

APPENDIX C
REVERSE KINEMATIC ANALYSIS NOTATION

The reverse kinematic analysis notation used in this thesis is defined as follows.

Subscripts h, i, j, k, and l are used where f=i-3, g=i-2, h=i-1, j=i+1, k=i+2, and l=i+3.

$$\begin{aligned} c_i &\equiv \cos\theta_i \\ s_i &\equiv \sin\theta_i \\ c_{ij} &\equiv \cos\alpha_{ij} \\ s_{ij} &\equiv \sin\alpha_{ij} \end{aligned} \tag{C.1}$$

$$\begin{aligned} X_j &\equiv s_{ij}s_j \\ Y_j &\equiv -\left(s_{jk}c_{ij} + c_{jk}s_{ij}c_j\right) \\ Z_j &\equiv c_{jk}c_{ij} - s_{jk}s_{ij}c_j \end{aligned} \tag{C.2}$$

$$\begin{aligned} \overline{X_j} &\equiv s_{jk}s_j \\ \overline{Y_j} &\equiv -\left(s_{ij}c_{jk} + c_{ij}s_{jk}c_j\right) \\ \overline{Z_j} &\equiv c_{ij}c_{jk} - s_{ij}s_{jk}c_j \end{aligned} \tag{C.3}$$

$$\begin{aligned} X_{ij} &\equiv X_i c_j - Y_i s_j \\ Y_{ij} &\equiv c_{jk}\left(X_i s_j + Y_i c_j\right) - s_{jk}Z_i \\ Z_{ij} &\equiv s_{jk}\left(X_i s_j + Y_i c_j\right) + c_{jk}Z_i \end{aligned} \tag{C.4}$$

$$\begin{aligned} X_{kj} &\equiv \overline{X_k}c_j - \overline{Y_k}s_j \\ Y_{kj} &\equiv c_{ij}\left(\overline{X_k}s_j + \overline{Y_k}c_j\right) - s_{ij}\overline{Z_k} \\ Z_{kj} &\equiv s_{ij}\left(\overline{X_k}s_j + \overline{Y_k}c_j\right) + c_{ij}\overline{Z_k} \end{aligned} \tag{C.5}$$

$$\begin{aligned} X_{ijk} &\equiv X_{ij}c_k - Y_{ij}s_k \\ Y_{ijk} &\equiv c_{kl}\left(X_{ij}s_k + Y_{ij}c_k\right) - s_{kl}Z_{ij} \\ Z_{ijk} &\equiv s_{kl}\left(X_{ij}s_k + Y_{ij}c_k\right) + c_{kl}Z_{ij} \end{aligned} \tag{C.6}$$

$$\begin{aligned} X_{kji} &\equiv X_{kj}c_i - Y_{kj}s_i \\ Y_{kji} &\equiv c_{hi}\left(X_{kj}s_i + Y_{kj}c_i\right) - s_{hi}Z_{kj} \\ Z_{kji} &\equiv s_{hi}\left(X_{kj}s_i + Y_{kj}c_i\right) + c_{hi}Z_{kj} \end{aligned} \tag{C.7}$$

$$
\begin{aligned}
X_{hijk} &\equiv X_{hij}c_k - Y_{hij}s_k \\
Y_{hijk} &\equiv c_{kl}\left(X_{hij}s_k + Y_{hij}c_k\right) - s_{kl}Z_{hij} \qquad \text{(C.8)} \\
Z_{hijk} &\equiv s_{kl}\left(X_{hij}s_k + Y_{hij}c_k\right) + c_{kl}Z_{hij} \\
X_{kjih} &\equiv X_{kji}c_h - Y_{kji}s_h \\
Y_{kjih} &\equiv c_{gh}\left(X_{kji}s_h + Y_{kji}c_h\right) - s_{gh}Z_{kji} \qquad \text{(C.9)} \\
Z_{kjih} &\equiv s_{gh}\left(X_{kji}s_h + Y_{kji}c_h\right) + c_{gh}Z_{kji} \\
X_{hijkl} &\equiv X_{hijk}c_l - Y_{hijk}s_l \\
Y_{hijkl} &\equiv c_{lm}\left(X_{hijk}s_l + Y_{hijk}c_l\right) - s_{lm}Z_{hijk} \qquad \text{(C.10)} \\
Z_{hijkl} &\equiv s_{lm}\left(X_{hijk}s_l + Y_{hijk}c_l\right) + c_{lm}Z_{hijk} \\
X_{lkjih} &\equiv X_{lkji}c_h - Y_{lkji}s_h \\
Y_{lkjih} &\equiv c_{gh}\left(X_{lkji}s_h + Y_{lkji}c_h\right) - s_{gh}Z_{lkji} \qquad \text{(C.11)} \\
Z_{lkjih} &\equiv s_{gh}\left(X_{lkji}s_h + Y_{lkji}c_h\right) + c_{gh}Z_{lkji} \\
U_{ij} &\equiv s_i s_{ij} \\
V_{ij} &\equiv -\left(s_j c_i + c_j s_i c_{ij}\right) \qquad \text{(C.12)} \\
W_{ij} &\equiv c_j c_i - s_j s_i c_{ij} \\
U_{ji} &\equiv s_j s_{ij} \\
V_{ji} &\equiv -\left(s_i c_j + c_i s_j c_{ij}\right) \qquad \text{(C.13)} \\
W_{ji} &\equiv c_i c_j - s_i s_j c_{ij} \\
U_{ijk} &\equiv U_{ij}c_{jk} - V_{ij}s_{jk} = U_{kji} \\
V_{ijk} &\equiv c_k\left(U_{ij}s_{jk} + V_{ij}c_{jk}\right) - s_k W_{ij} = V_{kji} \qquad \text{(C.14)} \\
W_{ijk} &\equiv s_k\left(U_{ij}s_{jk} + V_{ij}c_{jk}\right) + c_k W_{ij} = W_{kji} \\
U_{hijk} &\equiv U_{hij}c_{jk} - V_{hij}s_{jk} = U_{kjih} \\
V_{hijk} &\equiv c_k\left(U_{hij}s_{jk} + V_{hij}c_{jk}\right) - s_k W_{hij} = V_{kjih} \qquad \text{(C.15)} \\
W_{hijk} &\equiv s_k\left(U_{hij}s_{jk} + V_{hij}c_{jk}\right) + c_k W_{hij} = W_{kjih} \\
U_{ghijk} &\equiv U_{ghij}c_{jk} - V_{ghij}s_{jk} = U_{kjihg} \\
V_{ghijk} &\equiv c_k\left(U_{ghij}s_{jk} + V_{ghij}c_{jk}\right) - s_k W_{ghij} = V_{kjihg} \qquad \text{(C.16)} \\
W_{ghijk} &\equiv s_k\left(U_{ghij}s_{jk} + V_{ghij}c_{jk}\right) + c_k W_{ghij} = W_{kjihg} \\
U_{fghijk} &\equiv U_{fghij}c_{jk} - V_{fghij}s_{jk} = U_{kjihgf} \\
V_{fghijk} &\equiv c_k\left(U_{fghij}s_{jk} + V_{fghij}c_{jk}\right) - s_k W_{fghij} = V_{kjihgf} \qquad \text{(C.17)} \\
W_{fghijk} &\equiv s_k\left(U_{fghij}s_{jk} + V_{fghij}c_{jk}\right) + c_k W_{fghij} = W_{kjihgf}
\end{aligned}
$$

LIST OF REFERENCES

1. Carl D. Crane III and Joseph Duffy, *Kinematic Analysis of Robot Manipulators*, Cambridge University Press, New York, 1998.

2. W.H. ElMaraghy, H.A. ElMaraghy, A. Zaki, and A. Massoud, Design and Control of Robots with Flexibilities,*Annals of the CIRP*, Vol. 43/1/1994, p359-362.

3. W.D. Drotning, Sensor-Based Automated Docking of Large Payloads, *Proceedings, 38th Conference on Remote Systems Technology*, 1990, Volume 1, p 69-74.

4. Carl D. Crane III and Joseph Duffy, A Dynamic Analysis of a Spatial Manipulator to Determine Payload Weight, *Journal of Robotic Systems*, v 20, n 7, July 2003, p 355-371.

5. Yu-Wen Li, Jin-Song Wang, Li-Ping Wang, Stiffness Analysis of a Stewart Platform-Based Parallel Kinematic Machine, *Proceedings - IEEE International Conference on Robotics and Automation*, v 4, 2002, p3672-3677.

6. W. Khalil and D. Murareci, Kinematic analysis and singular configurations of a class of parallel robots, *Mathematics and Computers in Simulation*, v 41, n 3-4, Jul, 1996, p377-390.

7. Carl D. Crane III, Joseph Duffy and Julio C. Correa, Static Analysis of Tensegrity Structures Part 2. Numerical examples, *Proceedings of the ASME Design Engineering Technical Conference*, v 5 A, 2002, p 681-687.

8. K. Liu, F.L. Lewis and M. Fitzgerald, Solution of Nonlinear Kinematics of a Parallel-Link Constrained Steward Platform Manipulator, *Circuits, Systems, and Signal Processing*, v 13, n2-3, 1994, p167-183.

9. Dong Sun, James K. Mills and Yunhui Lui, Position Control of Robot Manipulators Manipulating a Flexible Payload, *The Interational Journal of Robotics Research*, Vol. 18, No. 3, March 1999, p 319-332.

10. Evangelos G. Papadopoulos, Large Payload Manipulation by Space Robots, *Proceedings of the 1993 IEEE/RSJ International Conference on Intelligent Robots and Systems*, 1993, p 2087-2094.

11. Dong Sun and Yun-Hui Lui, Position and Force Tracking of a Two-Manipulator System Manipulating a Flexible Beam Payload, *Proceedings – IEEE International Conference on Robotics and Automation*, v 4, 2001, p 3483-3488.

12. Dennis R. Jenkins, Space Shuttle: The History of the National Space Transportation System: The First 100 Missions, *Voyageur Press*, Stillwater, MN, 2001.

13. National Aeronautics and Space Administration, "John F. Kennedy Space Center Multimedia Gallery," http://mediaarchive.ksc.nasa.gov/index.cfm, October 2004.

14. Rockwell International, Lifting Fixture Set-OMS/RCS Pod H70-0679, The National Aeronautics and Space Administration, 1978.

15. Carl D. Crane III, Joseph Duffy, and Jose Rico. Screw Theory and its Application to Spatial Robot Manipulators, *Coursepack for EML 6282 Geometry of Mechanisms and Robots II*, Spring semester 2003.

BIOGRAPHICAL SKETCH

Jeff Brink graduated from the University of Michigan in December 2000 with Bachelor of Science degrees in Aerospace Engineering and Mechanical Engineering. Jeff started work at NASA in February 2001 as a systems engineer in shuttle processing at the Kennedy Space Center in Florida. In September 2001, he enrolled part-time in graduate school at the University of Central Florida. One year later, Jeff transferred to the University of Florida to study robotics. With the help of the University of Florida's distance learning program, FEEDS, Jeff will graduate in April 2005 with a Master of Engineering degree.